

Modeling biochar effects on soil organic carbon on croplands in ~~the MIMICS (MIcrobial-MIneral Carbon Stabilization)~~ a microbial decomposition model (MIMICS-BC v1.0)

Mengjie Han^{1,2,3}, Qing Zhao^{2,3,4}, Xili Wang⁶, Ying-Ping Wang⁷, Philippe Ciais⁸, Haicheng Zhang⁹, Daniel S. Goll⁸, Lei Zhu¹, Zhe Zhao¹, Zhixuan Guo¹, Chen Wang¹⁰, Wei Zhuang¹¹, Fengchang Wu¹², Wei Li^{1,5*}

¹Department of Earth System Science, Ministry of Education Key Laboratory for Earth System Modeling, Institute for Global Change Studies, Tsinghua University, Beijing 100084, China.

²Guangdong Key Laboratory of Integrated Agro-environmental Pollution Control and Management, Institute of Eco-environmental and Soil Sciences, Guangdong Academy of Sciences, Guangzhou 510650, China.

³Key Laboratory of Pollution Ecology and Environmental Engineering Institute of Applied Ecology; Institute of Applied Ecology, Chinese Academy of Sciences, Shenyang 110016, China.

⁴National-Regional Joint Engineering Research Center for Soil Pollution Control and Remediation in South China, Guangzhou 510650, China.

⁵Institute for Carbon Neutrality, Tsinghua University, Beijing 100084, China.

⁶Economic & Information center, Zhejiang, China.

⁷CSIRO Environment, Private Bag 10, Clayton South VIC 3169 Australia.

⁸Laboratoire des Sciences du Climat et de l'Environnement, LSCE/IPSL, CEA-CNRS-UVSQ, Université Paris Saclay, 91191, Gif sur Yvette, France.

⁹Sun Yat Sen Univ, Sch Geog & Planning, Guangzhou, Peoples R China.

¹⁰Key Laboratory of Vegetation Restoration and Management of Degraded Ecosystem, South China Botanical Garden, Chinese Academy of Sciences, Guangzhou, China.

¹¹Guangdong Institute of Engineering Technology Research Co., Ltd, Guangzhou 510440, China.

¹²State Key Laboratory of Environmental Criteria and Risk Assessment, Chinese Research Academy of Environmental Sciences, Beijing 100012, China.

*Correspondence to: Wei Li (wli2019@tsinghua.edu.cn)

Abstract. Biochar (BC) application in croplands aims to sequester carbon and improve soil quality, but its impact on soil organic carbon (SOC) dynamics is not represented in most land models used for assessing land-based climate mitigation, therefore we are unable to quantify the effect of biochar applications under different climate conditions or land management.

To fill this gap, here we implemented a submodel to represent biochar into a microbial decomposition model named MIMICS (MIcrobial-MIneral Carbon Stabilization). We first calibrate MIMICS with new representations of density-dependent microbial turnover rate, adsorption of available organic carbon on mineral soil particles, and soil moisture effects on decomposition using global field measured cropland SOC at ~~58-285~~ sites. We further integrate biochar in MIMICS resolving its effect on microbial decomposition and SOC sorption/desorption and optimize two biochar-related parameters in these processes using 134 paired SOC measurements with and without biochar addition. The MIMICS-biochar version can generally reproduce the short-term (≤ 6 yr) and long-term (8 yr) SOC changes after adding biochar (mean addition rate: 25.6 t ha⁻¹) ($R^2 = \underline{0.650.79}$ and $\underline{0.840.97}$) with a low root mean square error (RMSE = ~~3.613.73~~ and ~~3.316.08~~ g kg⁻¹). Our study incorporates

sorption and soil moisture processes into MIMICS and extends its capacity to simulate biochar decomposition, providing a useful tool to couple with dynamic land models to evaluate the effectiveness of biochar applications on removing CO₂ from the atmosphere.

1. Introduction

Soil organic carbon (SOC) is the largest terrestrial carbon pool, and increasing soil respiration in response to global warming can cause large carbon emissions to the atmosphere (Bond-Lamberty et al., 2018), ~~therefore add further constraint to stabilize future warming under 2 °C~~. On the other hand, SOC sequestration through improved land management practices has a potential to mitigate climate change by increasing soil carbon accumulation, such as the “4 per mille” project (Minasny et al., 2017).

Due to the limited temporal and spatial coverage of field SOC measurements, soil biogeochemical models have been widely applied to simulate SOC and its response to climate change and human activities (Eglin et al., 2010). Soil carbon models are evolving from first-order kinetics-based models with simple representation of pool sizes and their turnover rates to microbial models with explicit representation of microbial roles in SOC decomposition and stabilization (Manzoni & Porporato, 2009; Sulman et al., 2018). For example, the MIcrobial-MIneral Carbon Stabilization (MIMICS) model is a process-based soil carbon model with explicit representations of nonlinear SOC decomposition dynamics related to microbial physiology, substrate quality, and physical protection of SOC (Wieder et al., 2014; Wieder et al., 2015). This model has been calibrated with global SOC data and can well represent current understanding of SOC decomposition and formation (Wieder et al., 2015), and outperforms conventional first-order decomposition model in simulating spatial variation in SOC stocks in forest ecosystems on continental scale (Zhang et al., 2020). However, the model has not been evaluated for agricultural sites or misses processes that theoretically should influence SOC dynamics, ~~such as density dependent microbial processes, adsorption of available organic carbon or soil moisture effects~~.

The microbial interactions at the community level (e.g., competition) play a crucial role in controlling SOC dynamics, but they are not considered in many microbial models (Georgiou et al., 2017), resulting in unrestricted growth of microbial community size with more carbon input which is unrealistic (Buchkowski et al., 2017; Wieder et al., 2013). In addition, field experiments show that physicochemical adsorption plays a more important role in controlling DOC fluxes than the biodegradation process (Kalbitz et al., 2005). Although the adsorption mechanism is complex, depending on various factors such as pH, clay content, destruction and formation of soil aggregates (Mayes et al., 2012), some soil carbon models implemented dynamic adsorption and desorption processes controlled by DOC concentration and available mineral surface sites for binding (Wang et al., 2020; Wang et al., 2013). The availability of SOC is influenced by the adsorption process (Michalzik et al., 2003). Some adsorption kinetic equations, such as the Langmuir isotherm, have commonly been employed to

depict the adsorption/desorption process. However, the MIMICS model lacks consideration of the adsorption process, thus not effectively elucidating its role in stabilizing SOC. Furthermore, the effect of soil moisture on SOC cannot be ignored because it controls microbial activity, substrate availability and further influences soil respiration and nitrogen mineralization (Manzoni et al., 2012; Schimel et al., 2007). A set of empirical functions for the soil moisture effects were proposed for the use in earth system models (ESMs) (Moyano et al., 2013; Camino-Serrano et al., 2018), and a mechanistic moisture function that incorporates physicochemical and biological processes was also developed recently (Yan et al., 2018). In previous MIMICS versions, an implicit or explicit density dependent turnover was introduced (Wieder et al. 2015; Kyker-Snowman et al. 2020; Zhang et al., 2020; Georgiou et al. 2017), which cause an increase in biomass turnover with increasing microbial community size reflecting increasing pressure from competition for other resource other than carbon (e.g. space) and virus infections (Jansson and Wu, 2023), and a water scalar was used to represent the soil moisture effects (Wieder et al. 2019). The inclusion of density-dependent microbial turnover rate improved the accuracy of predicting SOC at the global scale compared to MIMICS without it and eliminated the correlation between simulated biases and input of annual litterfall (Zhang et al., 2020). MIMICS with soil water modifications showed comparable predicted global soil carbon stocks compared to other models, but to what extent soil water influences SOC turnover remains uncertain (Wieder et al., 2019). Therefore, based on these theories and model limitations, it is necessary to integrate the three aspects (density-dependent microbial turnover rate, adsorption/desorption processes, and soil moisture impacts) into one model version to improve the prediction accuracy of SOC dynamics. For agricultural lands, modeling the SOC decomposition processes is more challenging due to management practices such as tillage and fertilization, which can significantly interrupt carbon cycle and need specific parameterizations.

Biochar application in croplands as a soil amendment can improve the soil quality and increase the crop production (Smith, 2016; Woolf et al., 2010). Meanwhile, because biochar is produced from biomass through pyrolysis processes and is recalcitrant to be decomposed, it is also considered as a promising negative emission technology (NET) for climate mitigation (Fuss et al., 2018; Minx et al., 2018). The carbon dioxide removal (CDR) potential of biochar is estimated to be 0.5~2 GtCO₂e year⁻¹ (CO₂ equivalent) (Fuss et al., 2018; Minx et al., 2018). However, biochar application affects SOC mineralization through various processes (Palansooriya et al., 2019; Luo et al., 2017), resulting in positive or negative priming effects (PEs, changes of native SOC mineralization) (Zimmerman et al., 2011). A recent meta-analysis showed that biochar induced negative priming effects on average (-3.8%), but the 95% confidence interval (CI) of -8.1% to 0.8% also covers positive values (Wang et al., 2016a). Biochar may induce positive PEs through stimulating microbial activity by providing additional nutrients for soil microbes (El-Naggar et al., 2019; Li et al., 2019). Positive PEs usually occurred in shorter term (< 2 year), then decreased or changed to being negative over longer term (Luo et al., 2011; Singh & Cowie, 2014; Ding et al., 2017). For example, biochar can reduce SOC available for microbes by enhancing soil aggregate stability through associations between soil minerals and biochar (Zheng et al., 2018). Its porous structure and high surface area with strong adsorption affinity for SOC can thus cause

negative PEs (Zimmerman et al., 2011; Lehmann et al., 2021). PEs are also impacted by the properties of biochar (e.g., feedstock type, pyrolysis temperature) and soil climate (e.g., soil moisture) (Ding et al., 2017). Therefore, soil moisture could be closely related to the adsorption capacity of biochar, and needs to be included in the model for predicting PEs of biochar on SOC changes. The biochar decomposition and impacts on native SOC through priming effects are important for the CDR potential of biochar, but these processes are not represented in most land carbon models (Lehmann et al., 2021), precluding the model capacity of fully assessing the effectiveness of large-scale application of biochar as a NET and its environmental impacts.

In this study, we aim to improve the MIMICS model, one of few microbial-based soil carbon models that have been applied globally, by adding new processes controlling SOC dynamics, especially for cropland and develop a biochar model version that incorporates our current understanding of biochar effects on SOC for future predictions at the regional or global scale. We first added density-dependent microbial turnover rate, adsorption of available organic carbon, and soil moisture effects on microbial decomposition rate into MIMICS which are needed to simulate the response of SOC to biochar addition. The updated model versions were calibrated and validated using 285 field measured cropland SOC concentrations without biochar addition. We then accounted for biochar effects on SOC in MIMICS by calibrating two parameters related to biochar, using 134 paired field SOC measurements in short- and long-term with and without biochar addition.

2. Materials and methods

2.1 Observational data collection

~~We collected 387 paired field measurements of SOC concentrations (g kg^{-1}) in croplands with or without biochar addition from 58 locations (see the site map in Fig. S1) from published literatures. Soil properties (clay content (Clay), bulk density (BD), soil moisture (SM)), climatic conditions (mean annual temperature (MAT), mean annual precipitation (MAP)), biological variable (net primary productivity (NPP)) and biochar related characteristics: application rate (Rate_BC), the interval between biochar application and soil sampling (Age_BC), feedstock type (Feedstock_BC), pyrolysis temperature (Temp_BC) were also collected when available. Auxiliary information (e.g., location, and managements, crop cover types) and more detailed information can be found in Han et al. (2021).~~

~~Because some sites have multiple biochar addition experiments (e.g., pyrolysis temperature \times aging time of biochar), the control SOC concentrations at the same site were averaged, and the SOC concentrations with biochar addition for a given rate (Rate_BC) were also averaged, omitting other characteristics of the BC (like pyrolysis temperature). In total, 134 paired SOC data were used for model calibration (Fig. S1). The depth of soil sampled varies among sites, but is less than 30 cm in general.~~

The biochar application rate has a wide range of 0.9–120 t ha⁻¹ with a median value of 20 t ha⁻¹ (Fig. S2a). Most biochar addition experiments are short term with the median Age_{BC} of 1.2 year (Fig. S2b). The main types of cultivated crop are maize, rice and wheat.

We also used three published global SOC datasets for croplands without biochar addition (Sun et al., 2020; Geisseler et al., 2017; Zhou et al., 2017b) as independent datasets to evaluate the model performance for simulating cropland SOC in general. There are 227 sites in total in these three datasets (Fig. S1).

Soil properties that were not reported in the literature were extracted from gridded datasets using the coordinates of the sites: clay content from Global Soil Dataset for use in Earth System Models (GSDE, Shangguan et al., 2014) and SM from the satellite observations of Soil Moisture Active Passive (SMAP, Entekhabi et al., 2010). Missing soil BD in control treatments were filled according to the relationship between SOC and bulk density based on 4765 cultivated soil data from the 2nd national soil survey (Song et al., 2005), and a decrease of 7.6% (Omondi et al., 2016) from the control soil BD was assumed to fill the missing BD values in the biochar addition experiments. The climate variable MAT is extracted from WorldClim (Fick & Hijmans, 2017), and the mean annual aridity index (AI, i.e., precipitation/potential evapotranspiration) used in the soil moisture equation (Eq. 10) was obtained from the Global Aridity Index and Potential Evapotranspiration Database (Zomer et al., 2022). The biological variable (i.e., NPP) is from the MODIS NPP dataset (Zhao & Running, 2010).

2.2.1 Modifications of the MIMICS model

2.2.1.1 The default version of MIMICS (MIMICS-def)

The MIMICS model (Wieder et al., 2014; Wieder et al., 2015) includes two microbial functional groups, i.e. copiotrophic (r strategy) and oligotrophic (k strategy), and physiological tradeoffs between these two groups. The model explicitly considers the impacts of litter chemical quality by the partitioning of litter input into metabolic and structural litter carbon pools, and stable SOC formation through physical and physicochemical protection of microbial byproducts and leached litter carbon.

There are seven carbon pools in MIMICS including two litter pools, two microbial biomass pools and three SOC pools (Fig. 1). The litter inputs (LIT) are divided into metabolic (LIT_m) and structural pools (LIT_s) according to the litter quality (f_{met}, i.e., fraction of litter to LIT_m), which is linearly related to the ratio of lignin to nitrogen (lignin:N, Table S1). Microbial growth efficiency (MGE) determines the carbon fluxes from the two litter pools and the available SOC pool (SOC_a) for microbial biomass pools and heterotrophic respiration. The turnover of microbial biomass (τ) depends on the microbes functional types (MIC_r and MIC_k for r- and k-strategy, respectively). Three SOC pools represent the available (SOC_a), physically protected

(SOC_p) and chemically recalcitrant SOC (SOC_c). SOC in the protected pools (i.e., SOC_p and SOC_c) are released to the available SOC pool (SOC_a) over time. More detailed description of the model parameters and carbon fluxes can be found in Table S1 and Wieder et al. (2015). The carbon decomposition rate (mg C cm⁻³ hr⁻¹) of the litter and SOC pools is based on a temperature-sensitive Michaelis–Menten kinetics (Allison et al., 2010; Schimel & Weintraub, 2003):

$$165 \quad \frac{dC_s}{dt} = MIC \times \frac{V_{max} \times C_s}{K_m + C_s} \quad (1)$$

where C_s (mg C cm⁻³) is the size of a substrate carbon pool (LIT or SOC), and MIC (mg C cm⁻³) is the size of the microbial carbon pool (MIC_r or MIC_k). V_{max} and K_m are the microbial maximum reaction velocity (mg C (mg MIC)⁻¹ hr⁻¹) and the half-saturation constant (mg C cm⁻³), respectively, which depend on temperature, T, in °C.

$$V_{max} = e^{V_{slope}T + V_{int}} \times a_v \times V_{mod} \quad (2)$$

$$170 \quad K_m = e^{K_{slope}T + K_{int}} \times a_k \times K_{mod} \quad (3)$$

where V_{mod} and K_{mod} represent the modifications of V_{max} and K_m based on their dependence on litter quality, microbial functional types, and soil texture. a_v and a_k are the tuning coefficients of V_{max} and K_m, respectively. V_{slope} and K_{slope} are the regression coefficients, and V_{int} and K_{int} are the regression intercepts.

175 The turnover of MIC_r and MIC_k (MIC_τ, mg C cm⁻³ hr⁻¹) at each time step depends on their specific turnover rate (k_{mic}, hr⁻¹), annual total litter input (LIT_{tot}, g C m⁻² year⁻¹) and f_{met}:

$$MIC_{\tau} = a_{\tau} \times k_{mic} \times e^{c f_{met}} \times \max(\min(\sqrt{LIT_{tot}}, 1.2 \sqrt{LIT_{tot}, 1.2}), 0.8) \times MIC \quad (4)$$

where a_τ (=1.0, dimensionless) is the tuning coefficient of k_{mic}. c is the regression coefficient of MIC_r (0.3) and MIC_k (0.1). The

180 carbon inputs from microbial biomass to SOC pools are determined by the microbial biomass turnover.

The carbon transfer from SOC_p to SOC_a (D, mg C cm⁻³ hr⁻¹) represents the ~~deprotection~~desorption of SOC_p from mineral surfaces or the breakdown of aggregates, calculated as a function of soil clay content (f_{clay}):

$$D = 1.5 \times 10^{-5} \times k_d \times e^{-1.5 f_{clay}} \quad (5)$$

185 where k_d (=1.0, dimensionless) is a tuning coefficient of the ~~deprotection~~desorption rate. The parameter values of the default MIMICS version can be found in Table S1.

2.21.2 MIMICS considering density-dependent microbial turnover rate (MIMICS-T)

Similar to the logistic growth model in population ecology, various regulatory mechanisms (e.g., competition, virus) can

limit microbial population size (Buchkowski et al., 2017, Jansson and Wu, 2023). The absence of restrictions on population
 190 size other than carbon result in predictions of microbial biomass increasing indefinitely with carbon inputs. Consequently,
 the response of predicted SOC to changes in carbon inputs is close to zero which contradicts field observations (Georgiou et
 al., 2017). A density dependent turnover rate with $\beta > 1$ was adopted to regulate the responses of soil microbial biomass to
 external environment variations, such as carbon input, thereby SOC dynamics in previous microbial models (Georgiou et al.,
 2017, Zhang et al., 2017). We incorporated the density-dependent microbial turnover rate into MIMICS following Georgiou et
 195 al. (2017) and Zhang et al. (2020). In the MIMICS-T version, we modified Eq. 4 to represent the increased microbial turnover
 rate with growing microbial biomass density (MIC, mg C cm⁻³):

$$MIC_{\tau} = a_{\tau} \times k_{mic} \times e^{c \times f_{met}} \times \max(\min(\sqrt{LIT_{tot}}, 1.2 \sqrt{LIT_{tot} - 1.2}), 0.8) \times MIC^{\beta}$$

(6)

where β is the density-dependence exponent.

200 2.21.3 MIMICS-T with additional representation of sorption (MIMICS-TS)

Although the MIMICS model can simulate the desorption process (the yellow arrow from SOC_p to SOC_a, Fig. 1), the
 adsorption process is still missing. In the original version of MIMICS, fixed fractions of litter and microbial turnover are
 transferred to the physically protected SOC pool (SOC_p, Fig. 1), the SOC_p is then deprotected from mineral surfaces or
 breakdown of aggregates using a desorption rate which is a function of clay fraction. Therefore, we do not think that the
 205 original MIMICS actually simulate sorption as a process, as sorption is dependent on substrate concentration, therefore the
 sorption rate should vary with dissolved organic carbon concentration, rather than being proportional to microbial carbon
 turnover rate as assumed in the original MIMICS. Therefore, ~~We then~~ we further added the adsorption of available SOC into
 MIMICS following Wang et al. (2013) and Mayes et al. (2012). The MIMICS-TS version includes a new sorption process (the
 purple arrow from SOC_a to SOC_p in Fig. S31) but keeps the original desorption process (i.e., the yellow arrow from SOC_p to
 210 SOC_a in Fig. S31) unchanged. The sorption capacity of SOC_a (Q_{max}) increases with increasing clay content, and the carbon flux
 of the sorption process is calculated as follows:

$$F_{ads} = K_{ads} \times \left(1 - \frac{SOC_p}{Q_{max}}\right) \times SOC_a \quad (7)$$

$$K_{ads} = k_d \times k_{ba} \quad (8)$$

$$Q_{max} = 10^{(c_1 \times \log(\%clay) + c_2)} \quad (9)$$

215 where F_{ads} is the carbon flux from SOC_a to SOC_p (mg C cm⁻³ hr⁻¹). k_{ba} is the binding affinity, and K_{ads} is the sorption rate of
 SOC_p which is associated with the ~~deprotection~~ desorption rate (k_d). Q_{max} is the maximum sorption capacity of SOC_p (mg C cm⁻³
 soil). c_1 and c_2 are the coefficient for estimating Q_{max} from Mayes et al. (2012).

2.21.4 MIMICS-TS with soil moisture effects (MIMICS-TSM)

Finally, based on MIMICS-TS, we added soil moisture effects on decomposition into MIMICS. We tested two empirical functions for soil moisture used respectively in the Century model (Parton et al., 2000, Eq. 10) and the ORCHIDEE-SOM model (Camino-Serrano et al., 2018, Eq. 11). We also attempted to implement one mechanism-based function that captures the main physicochemical and biological processes of soil moisture in regulating soil respiration from Yan et al. (2018) (Eq. 12). The three functions of soil moisture are illustrated in Fig. S4S1.

$$f_{m1}(w) = \frac{1}{1+p_1 \times e^{(p_2 \times w)}} \quad (10)$$

$$f_{m2}(\theta) = \max(0.25, \min(1, k_1 \times \theta^2 + k_2 \times \theta + k_3)) \quad (11)$$

$$f_{m3}\left(\frac{\theta}{\varphi}\right) = \begin{cases} \frac{K_{\theta} + \theta_{op}}{K_{\theta} + \theta} \times \left(\frac{\theta}{\theta_{op}}\right)^{(1+an_s)}, & \theta < \theta_{op} \\ \left(\frac{\varphi - \theta}{\varphi - \theta_{op}}\right)^b, & \theta \geq \theta_{op} \end{cases} \quad (12)$$

where f_{mi} ($i=1, 2, 3$, unitless value in range from 0 to 1) is the response factor to soil moisture. w is the soil moisture indicator (AI, mm mm^{-1}). p_1 and p_2 are empirical parameters of soil moisture scalar with $p_1 = 30$ and $p_2 = -8.5$ (Parton et al., 2000). θ is soil moisture ($\text{m}^3 \text{m}^{-3}$). k_1 , k_2 and k_3 are soil moist coefficients with 1.1, 2.4 and 0.29, respectively (Camino-Serrano et al., 2018). φ is the soil porosity related to soil bulk density, and θ/φ is the relative water content in soil pores. θ_{op} is an optimum soil moisture content parameter at which the heterotrophic respiration rate peaks. K_{θ} is moisture constant depending on organic-mineral associations. n_s is saturation exponent depending on soil structure and texture. a and b are SOC-microbial collocation factor and oxygen supply restriction factor, respectively (Yan et al., 2018).

We assumed that the kinetic parameters V_{max} and K_m respond to soil moisture, similarly to temperature in Michaelis-Menten equation by affecting enzyme activity and enzyme-substrate affinity, respectively. The soil enzyme-substrate affinity was found to increase with soil moisture due to the increased diffusion and movement of substrate, but the affinity may also decrease due to decreased substrate concentrations (Zhang et al., 2009). Thus, we translated the impacts of soil moisture on the enzyme-substrate affinity to changes in K_m . In MIMICS-TSM, the effects of soil moisture on SOC decomposition rate are represented through multiplying the response factor by V_{max} and K_m as follows (Eq. 13, 14).

$$V_{max} = e^{V_{slope} \cdot T + V_{int}} \cdot a_v \cdot V_{mod} \times f_{mi} \quad (13)$$

$$K_m = e^{K_{slope} \cdot T + K_{int}} \cdot a_k \cdot K_{mod} \times f_{mi} \quad (14)$$

The MIMICS models with three soil moisture functions of f_{m1} (Eq. 10), f_{m2} (Eq. 11) and f_{m3} (Eq. 12) are indicated as MIMICS-TSM_a, MIMICS-TSM_b and MIMICS-TSM_c, respectively. The modifications of all MIMICS versions are summarized in Table S21. ~~There are only minor differences in the accuracy of reproducing SOC observation among the three~~

versions (Fig. S11).

Because the MIMICS TSM₆ version with the sorption process and soil moist effects has the best accuracy in reproducing the observations (see Section 3.1 and Fig. 2), this version was used for further implementation of biochar effects on SOC.

250 2.2.1.5 Adjusted parameters for cropland SOC

Crop NPP at each site was used as the litter input to soil, but different crop types (e.g., maize, rice and wheat) were not specified in the model. The leaf, root and stem litter were assumed as a fixed fraction of crop NPP. The ratio of carbon to nitrogen (C: N) and the ratio of lignin to carbon (lignin: C) of leaf, root, and stem (Table S2) were used to calculate the metabolic fraction in the total crop litter (f_{met}). The metabolic fraction in the total crop litter (f_{met}) It is calculated as the mean
255 metabolic fractions in leaf, root and ~~wood~~stem, weighted by NPP in the three parts. In order to adapt MIMICS for simulating cropland SOC, we modified ~~the ratio of carbon to nitrogen (C:N)~~ and ~~the ratio of lignin to carbon (lignin:C)~~ in the three parts based on field measurements of main crop types (Abiven et al., 2005, Table S3S2). ~~The derived ratio of lignin to nitrogen (Lignin:N) is used to determine f_{met} (Table S1).~~ A harvest index (HI) of 0.45 (Hicke & Lobell, 2004) was also applied to remove the harvested part of crop and obtain the litter input to soil (= crop aboveground NPP × (1-HI)).

260 2.3.2 Implementing biochar modeling in MIMICS

When applying biochar in croplands, a fraction of biochar ($f_{loss} = 2\%$, Archontoulis et al., 2016) is assumed to be lost during application. Although biochar is recalcitrant to decompose with a long turnover time (556 ± 484 yr) in general, it contains some labile fraction (108 ± 196 day), and its stability varies with different biochar feedstocks, pyrolysis temperatures and soil properties (Wang et al., 2016a). Because the sizes of SOC_p and SOC_c pools in MIMICS were not measured directly in

265 the field studies, the 98 % remaining fraction is partitioned into three MIMICS SOC pools by assuming 60% goes to SOC_p based on the measured proportions of added biochar within aggregates (Yoo et al., 2017), 20% goes to SOC_a according to the labile C portion in biochar (Roberts et al., 2010) and 20% goes to SOC_c, respectively (Fig. 1). Note that biochar is not treated as a separate carbon pool but assumed to mix with other carbon in existing pool (Fig. 1). In addition to the increase of total SOC, some important processes controlling SOC accumulation and decomposition are affected by biochar addition. We thus
270 modified the parameters related to decomposition and ~~deprotection~~desorption of SOC (Fig. 1). The associated rationales, equations and parameters are described in the following sections.

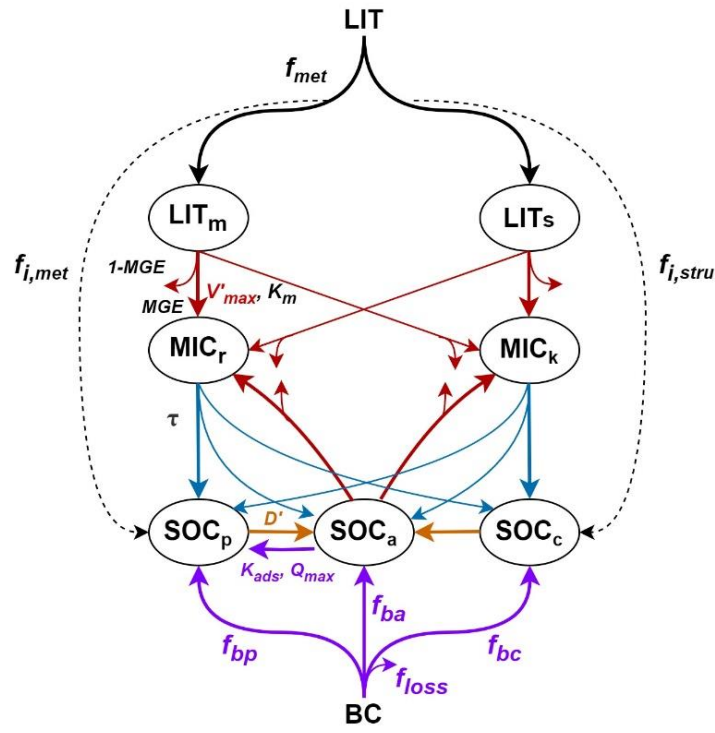


Fig. 1 Framework of the MIMICS model with biochar addition (MIMICS-BC; adapted from Wieder et al. (2015)). The turnover of microbial biomass (τ , blue arrows) is modified with density-dependent microbial turnover rate (Eq. 6, MIMICS-T). The adsorption process of SOC_p to SOC_a (purple arrow) is newly added and is associated with the adsorption rate (K_{ads}) and the maximum sorption capacity (Q_{max}) (Eq. 7-9, MIMICS-TS). The carbon decomposition processes (red arrows) are modified further with three soil moisture scalars that are applied to microbial maximum reaction velocity (V_{max}) and the half-saturation constant (K_m) (Eq. 10-12, MIMICS-TSM_a, MIMICS-TSM_b, MIMICS-TSM_c). When biochar is added to soil, the biochar (BC) carbon with an assumed fraction loss (f_{loss}) is partitioned into SOC_p, SOC_a and SOC_c based on f_{bp} , f_{ba} and f_{bc} , respectively (purple arrows from BC to SOC pools). The desorption process (orange arrow from SOC_p to SOC_a) is modified through changes in the desorption rate of SOC_p (D') with biochar addition. The carbon decomposition processes (red arrows) are modified by adjusting the microbial maximum reaction velocity (V'_{max}) with biochar addition.

Fig. 1 Framework of the MIMICS model with biochar addition (MIMICS-BC; adapted from Wieder et al. (2015)). The biochar (BC) carbon with a fraction loss (f_{loss}) is partitioned into SOC_p, SOC_a and SOC_c based on f_{bp} , f_{ba} and f_{bc} , respectively. The modified processes with biochar addition are marked with colors, and the purple arrows represent the newly added processes. The deprotection process (orange arrow) is modified through changes in the deprotection rate of SOC_p (D') with biochar addition. The adsorption process (purple arrow) is associated with the adsorption rate (K_{ads}) and the maximum sorption capacity (Q_{max}). The carbon decomposition processes (red arrows) are modified by adjusting the microbial maximum reaction velocity (V'_{max}) with biochar addition. The description of other unmodified processes in the default MIMICS model version can be found in Fig. S3.

295 The negative priming effects of biochar addition on SOC may be caused by the inhibition of microbial activity due to changes in the soil environments by biochar, or by the SOC protection against microbial utilization through mineral adsorption or aggregates (Zimmerman et al., 2011). We assumed that biochar addition decreased the mineralization of native SOC (negative PE) because of its porous structure and strong adsorption affinity to organic matter (Kasozi et al., 2010), which was reported to have significantly contributed to the negative PE mechanism from biochar addition (Zheng et al., 2018; Zimmerman et al., 2011). We assumed that biochar addition decreases the mineralization of native SOC (negative PE) because of its strong adsorption affinity for organic matter (Lehmann et al., 2021). A ~~deprotection~~desorption coefficient (f_d , ha t⁻¹ Rate_{BC}) was defined as a function of the biochar application rate (Rate_{BC}) based on Woolf & Lehmann (2012) and Archontoulis et al. (2016), and Eq. 5 was thus modified as:

$$D' = D \times (1 + f_d \times Rate_{BC} \times BC_C)$$

(15)

305 where D' (mg C cm⁻³ hr⁻¹) is the new ~~deprotection~~desorption rate of SOC_p with biochar addition, and a negative value of f_d indicates a negative priming effect. The Rate_{BC} is the application rate of biochar (t BC ha⁻¹) and BC_C is the carbon content in biochar (t C t⁻¹BC). Because the adsorption and desorption of SOC are interrelated dynamic process, modification of the desorption process with biochar addition also impacts the adsorption process. Therefore, we only modified f_d in Eq. (15) to represent the negative PE of biochar.

310 We also assumed that biochar provides nutrients (e.g., nitrogen and phosphorus) to microbes and stimulate microbial growth and activity, inducing a positive PE to SOC (El-Naggar et al., 2019). We defined a new decomposition rate coefficient (f_v , ha t⁻¹ Rate_{BC}) that is a function of Rate_{BC}, and included it in MIMICS by modifying Eq. 2:

$$V'_{max} = V_{max} \times (1 + f_v \times Rate_{BC} \times BC_C)$$

315 (16)

where V'_{max} is the new microbial maximum reaction velocity (mg C (mg MIC)⁻¹ hr⁻¹) with biochar addition.

Biochar may also have a positive priming effect on SOC by increasing the degradation rate of available SOC by microbes (i.e., SOC_a in MIMICS). Therefore, we added a test through modifying the V_{max} as a function of biochar addition rate only in the fluxes from SOC_a to MIC_r and MIC_k, instead of in all fluxes of decomposition (Eq. 16, red arrows in Fig. 1).

2.4.3 Parameter optimization and model evaluation Model calibration and evaluation

2.3.1 Observational data collection

325 We collected 387 paired field measurements of SOC concentrations (g kg^{-1}) in croplands with or without biochar addition from 58 locations (see the site map in Fig. 2) from published literatures. Soil properties (clay content (Clay), bulk density (BD), soil moisture (SM)), climatic conditions (mean annual temperature (MAT), mean annual precipitation (MAP)), biological variable (net primary productivity (NPP)) and biochar-related characteristics: application rate (Rate_BC), the interval between biochar application and soil sampling (Age_BC), feedstock type (Feedstock_BC), pyrolysis temperature (Temp_BC) were also collected when available. Auxiliary information (e.g., location, and managements, crop types) and more detailed information can be found in Han et al. (2021).

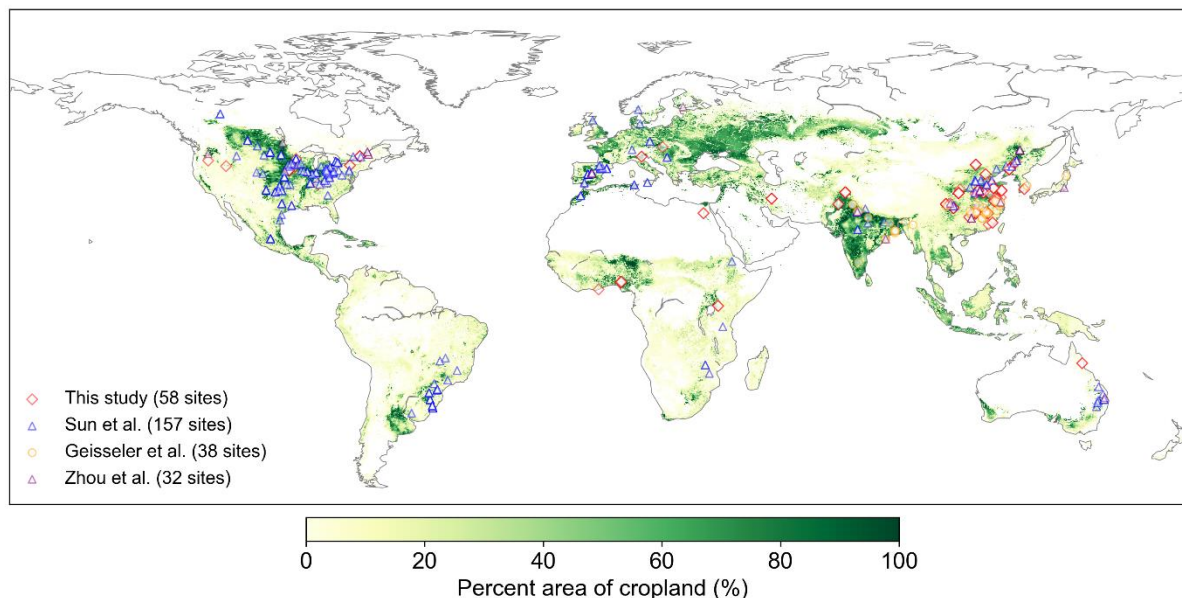
330 Because some sites have multiple biochar addition experiments (e.g., pyrolysis temperature \times aging time of biochar), the control SOC concentrations at the same site were averaged, and the SOC concentrations with biochar addition for a given rate (Rate_BC) were also averaged, omitting other characteristics of the BC (like pyrolysis temperature). In total, 134 paired SOC data were used for model calibration (Fig. 2). The depth of soil sampled varies among sites, but is less than 30 cm in general.

335 The biochar application rate has a wide range of 0.9~120 t ha^{-1} with a median value of 20 t ha^{-1} (Fig. S2a). Most biochar addition experiments are short-term with the median Age_BC of 1.2 year (Fig. S2b). The main types of cultivated crop are maize, rice and wheat.

340 There are SOC measurements on cropland sites from 58 control treatments (no BC application) and 134 measurements from biochar treatments at the 58 sites. One control treatment may correspond to multiple biochar treatments with different applied biochar rates at a single site. Considering the 58 site observations may be inadequate to constrain all the new features in the revised model, we also collected SOC data on croplands (no biochar addition) from other three published global datasets (227 sites in total, Sun et al., 2020; Geisseler et al., 2017; Zhou et al., 2017b). Therefore, 285 sites in total were used to calibrate and evaluate the model performance for simulating cropland SOC without biochar addition (Fig. 2).

345 Soil properties that were not reported in the literature were extracted from gridded datasets using the coordinates of the sites: clay content from Global Soil Dataset for use in Earth System Models (GSDE, Shangguan et al., 2014) and SM from the satellite observations of Soil Moisture Active Passive (SMAP, Entekhabi et al., 2010). Missing soil BD in control treatments were filled according to the relationship between SOC and bulk density based on 4765 cultivated soil data from the 2nd

350 national soil survey (Song et al., 2005), and a decrease of 7.6% (Omondi et al., 2016) from the control soil BD was assumed to fill the missing BD values in the biochar addition experiments. The climate variable MAT is extracted from WorldClim (Fick & Hijmans, 2017), and the mean annual aridity index (AI, i.e., precipitation/potential evapotranspiration) used in the soil moisture equation (Eq. 10) was obtained from the Global Aridity Index and Potential Evapotranspiration Database (Zomer et al., 2022). The biological variable (i.e., NPP) is from the MODIS NPP dataset (Zhao & Running, 2010).



355

Fig. 2 Locations of field cropland SOC measurements with or without biochar addition collected in this study and SOC measurements without biochar addition from Sun et al. (2020), Geisseler et al., (2017) and Zhou et al., (2017b). Number of sites is also shown in the legend. Note that one site may have multiple paired SOC data due to various experimental conditions of biochar addition in our collected 58 sites. The cropland area percentage in each 10 km × 10 km grid cell is derived from EarthStat (<http://www.earthstat.org>; Ramankutty et al., 2008).

360

2.3.2 Calibration and validation for MIMICS versions without biochar

All field SOC observations in the control treatments (without biochar) from the paired measurements and SOC from the other three global datasets (Fig. 2) were assumed at a steady state, which is under present climate and continuous input of crop NPP after 45% removal of grain with a specific crop litter quality (Section 2.1.5, Table S2).

365

All field SOC observations in control plots were assumed at a steady state. SOC pools in MIMICS reached an equilibrium state after about 200 years of model run (Fig. S3). To accelerate this process, we used New-Ralphson method (Press et al., 2007) to obtain the steady SOC state with the site-level inputs of annual mean crop NPP, MAT, Clay, SM and BD in the parameter optimization. This approach is constructed based on the fundamental principles governing biogeochemical cycle processes in terrestrial ecosystems (e.g., respiration, carbon distribution). A set of first-order ordinary differential equations were built to express the dynamics of carbon flows in soil over time and it can be solved numerically to obtain steady carbon pool sizes (see codes for further details in Code availability).

370

The Shuffled Complex Evolution Algorithm (SCE-UA) has been proven to be a robust method for parameter optimization (Duan et al., 1994; Muttill & Jayawardena, 2008), and the SCE-UA method from the *spotpy* package in python (Houska et al., 2015; <https://pypi.org/project/spotpy/>) was applied here. Parameters are optimal when the root mean square error (RMSE, Eq. 17) between simulated SOC and observed SOC concentrations is minimized. The Akaike information

375 criterion (AIC, Eq. 18, Akaike, 1974), which considers both model error and the number the model parameters, was also
calculated to evaluate different MIMICS versions.

$$RMSE = \sqrt{\frac{\sum_{i=1}^n (SOC_{obs,i} - SOC_{sim,i})^2}{n}} \quad (17)$$

$$AIC = n \times \ln \left(\frac{\sum_{i=1}^n (SOC_{obs,i} - SOC_{sim,i})^2}{n} \right) + 2p \quad (18)$$

Where $SOC_{obs,i}$ and $SOC_{sim,i}$ are the observed and simulated SOC at each i site. n is the number of observations, and p is the
380 number of model parameters to be optimized.

The parameters optimized in different MIMICS versions using the entire SOC dataset (i.e., ~~58-285~~ sites) are shown in Table
~~S4S3. Soil depth was not explicitly considered in this study, and we assumed that the soil carbon concentrations (g kg⁻¹) are
similar within the top 30 cm.~~ Note that the parameters of soil moisture functions (Eq. 10-12) are directly derived from the
385 original literature (Parton et al., 2000; Camino-Serrano et al., 2018; Yan et al., 2018) and not optimized in MIMICS-TM. We
validated the models against our datasets including SOC and auxiliary information (Fig. ~~S12~~) for the main crop types (maize,
rice, and wheat), and the relationships between SOC in these crop types and model input variables (i.e., NPP, MAT, Clay) were
analyzed. ~~The MIMICS model can run for each site, but to be consistent with the model input resolution of daily temperature in
the transient simulation, the resolution of 0.5° was used for site aggregation. In detail, all sites within a given grid cell of 0.5° ×
390 0.5° were aggregated on average, and the averaged value was used to compare the model result in this grid cell. In addition, all
the site SOC data within 0.5° × 0.5° grid cell were aggregated to match the resolution of model simulations.~~ We also conducted
a sensitivity test of MIMICS input variables (i.e., MAT, Clay, NPP, SM and BD) with four perturbation levels of -50%, -25%,
25% and 50% to explore the effects of possible underrepresented processes on the cropland steady SOC.

395 ~~We randomly separated 80% of all the 285 sites for parameter optimization, and 20% for MIMICS versions (MIMICS-def,
MIMICS-T, MIMICS-TS and MIMICS-TSM_b) validation. The R², RMSE and AIC were calculated by comparing simulated
SOC with the observed SOC in training and test datasets. The cross-validation was also used to evaluate each model version
(i.e., MIMICS-def, MIMICS-T, MIMICS-TS, MIMICS-TSM_b) by randomly selecting 80% data for parameter optimization,
and the remaining 20% data for model evaluation. The random selection is repeated for 10 times, and the mean R², RMSE and
400 AIC were calculated by comparing simulated SOC with the observed SOC in test datasets.~~

2.3.3 Calibration and validation for MIMICS versions with biochar (MIMICS-BC)

For the version of MIMICS with biochar addition, we run ~~for each site~~ parallel simulations with control (without biochar
addition) and experimental simulation (with biochar addition) for Age_BC year at hourly time steps, restarted from the

previous SOC equilibrium. Not that these simulations for biochar addition are transient runs and thus SOC is not in a steady state. In order to meet the daily time step of transient runs required by MIMICS, the two model runs were forced by 6-hour surface temperature at a grid box where the site was located from Climatic Research Unit and Japanese reanalysis data (CRU-JRA, Kobayashi et al., 2015; Harris et al., 2014), which can differ from WordClim (time resolution: year) used in Section 2.3.1. The two model runs are forced by site level 6-hour temperature data from Climatic Research Unit and Japanese reanalysis data (CRU-JRA, Kobayashi et al., 2015; Harris et al., 2014) and NPP derived from MODIS (Zhao & Running, 2010).

410 The soil-related inputs of Clay, SM and BD are assumed invariant in time and consistent with input data for the steady SOC runs. The absolute SOC changes (ΔSOC , g kg⁻¹, Eq. 19) in the simulated and observed SOC concentrations were compared after BC addition. The RMSE between simulated and observed ΔSOC was minimized using SCE-UA for parameter optimization. AIC and the slopes of regression lines between the simulated and observed SOC changes were analyzed.

$$\Delta SOC = X_t - X_c \quad (19)$$

415 where X_t and X_c is the observed (or simulated) SOC concentrations with and without biochar addition, respectively.

The 134 paired observations were randomly split into training samples for parameter optimization (80% data) and test samples for model validation (20% data). Four tests were conducted to evaluate the performance of MIMICS_{TSMb-BC} on simulating SOC changes after biochar addition using the optimized parameters values in MIMICS-TSM_b (i.e., $a_v, a_h, k_d, \beta, k_{ba}, c_1, c_2$; Table S3): 1) without biochar-related parameters; 2) with only one new biochar-related parameter (i.e., the desorption coefficient, f_d , Eq. 15) optimized (MIMICS_{TSMb-BCD}); 3) with two new biochar-related parameters (i.e., f_d and the decomposition rate coefficient, f_y , Eq. 16) optimized in all decomposition processes (MIMICS_{TSMb-BCDV}); 4) with two new biochar-related parameter (i.e., f_d and f_y) optimized only in the fluxes from SOC_a to MIC pools (MIMICS_{TSMb-BCDV-SOCa}). Although MIMICS-TSM_b is not the model with the highest R² and lowest RMSE and AIC, the differences of R², RMSE and AIC among various versions are relatively small (Fig. S5). The new processes (density dependent processes, sorption, and soil moisture scalars) are based on theoretical understanding and have shown to improve predictions of soil carbon in previous studies (Zhang et al., 2020, Liang et al., 2019, Abramoff et al. 2022). Thus, this version was used for further development of biochar processes in MIMICS. As an alternative model version, we also tested implementation of biochar processes in MIMICS-T that have a highest R² and lowest RMSE and AIC in model validation (Fig. S5b). The model versions and simulation settings are shown in Table 1 and Fig. 3, and the optimized parameters values in these tests are shown in Table S3.

~~Three tests were conducted to evaluate the performance of MIMICS-BC on simulating SOC changes after biochar addition using the optimized parameters values in MIMICS-TSM_b (i.e., $a_v, a_h, k_d, \beta, k_{ba}, c_1, c_2$; Table 1): 1) without biochar related parameters; 2) with only one new biochar related parameter (i.e., the deprotection coefficient, f_d , Eq. 15) optimized (MIMICS-BC_D); 3) with two new biochar related parameters (i.e., f_d and the decomposition rate coefficient, f_y , Eq. 16) optimized (MIMICS-BC_{DV}). The~~

435 optimized parameters values in these three tests are shown in Table 1.

Considering the uncertainties in the MIMICS-BC parameters, we conducted a sensitivity test of biochar-related parameters (i.e., f_d, f_v, f_{bp}, f_{ba}) and input variables (i.e., Rate_BC, Age_BC, NPP, Clay, SM) with four perturbation levels of -50%, -25%, 25% and 50% for each site. Because the duration of most biochar addition experiments is short (74.2% data < 3 years), we also extracted data with Age_BC \geq 3yr (4 yr, 5 yr and 6 yr) and tested the model performance on them separately. Due to lack of field measured data for a longer period, we extended our collected control SOC data to 8 years according to the decomposition curve of biochar in soil fitted by a double first-order exponential decay model (Fig. S6S4; Wang et al., 2016a). Note that the double exponential decay function is only applied to the observational records of measurement data, and the function itself is not used in the MIMICS model. Specifically, the 8-yr SOC data with biochar addition is the sum of field control SOC observations and the residual biochar carbon in soil after 8 years. These extended long-term data were also used for parameter optimization and model evaluation. The relationships between observed Δ SOC and model input variables and the partial correlations between biases (simulated minus observed Δ SOC) from the three tests and model input variables (soil-, climate-, biological-, and biochar-related variables) were also analyzed to detect the possible missing processes.

445 Table 1 Modifications in various MIMICS versions.

<u>Model</u>	<u>Model version</u>	<u>Description</u>
<u>MIMICS</u>	<u>MIMICS-def</u>	<u>The default model version with modified parameters related to crop properties (Section 2.1.5).</u>
	<u>MIMICS-T</u>	<u>Considering the density-dependent microbial turnover rate (denoted as “T”, Eq. 6).</u>
	<u>MIMICS-TS</u>	<u>Adding the sorption process of SOC_p based on MIMICS-T (“S”, Eq. 7-9).</u>
	<u>MIMICS-TSM_a</u>	<u>Including soil moisture effects from CENTURY model (“M_a”) based on MIMICS-TS.</u>
	<u>MIMICS-TSM_b</u>	<u>Including soil moisture effects from ORCHIDEE-SOM model (“M_b”) based on MIMICS-TS.</u>
	<u>MIMICS-TSM_c</u>	<u>Including soil moisture effects from Yan et al. (2018) (“M_c”) based on MIMICS-TS.</u>
<u>MIMICS_{T-BC}</u>	<u>MIMICS-T</u>	<u>Including the density-dependent microbial turnover rate but without biochar-related parameters for biochar addition.</u>
	<u>MIMICS_{T-BCD}</u>	<u>Including biochar effects on SOC by modifying desorption rate of SOC_p in MIMICS-T (Eq. 15).</u>
	<u>MIMICS_{T-BCDV}</u>	<u>Including further biochar effects on SOC by modifying the microbial maximum reaction velocity in all decomposition processes in MIMICS-T (Eq. 16).</u>
	<u>MIMICS_{T-BCDV-SOC_a}</u>	<u>Including further biochar effects on SOC by modifying the microbial maximum reaction velocity only in microbial decomposition of SOC_a in MIMICS-T (Eq. 16).</u>
<u>MIMICS_{TSM_b-BC}</u>	<u>MIMICS-TSM_b</u>	<u>Including the density-dependent microbial turnover rate, the sorption process and soil moisture effects but without biochar related parameters for biochar addition.</u>
	<u>MIMICS_{TSM_b-BCD}</u>	<u>Similar to MIMICS_{T-BCD} but biochar is added in MIMICS-TSM_b.</u>

MIMICS_{TSMb-BCDV}

Similar to MIMICS_{T-BCDV} but biochar is added in MIMICS-TSM_b.

MIMICS_{TSMb-BCDV-SOCa}

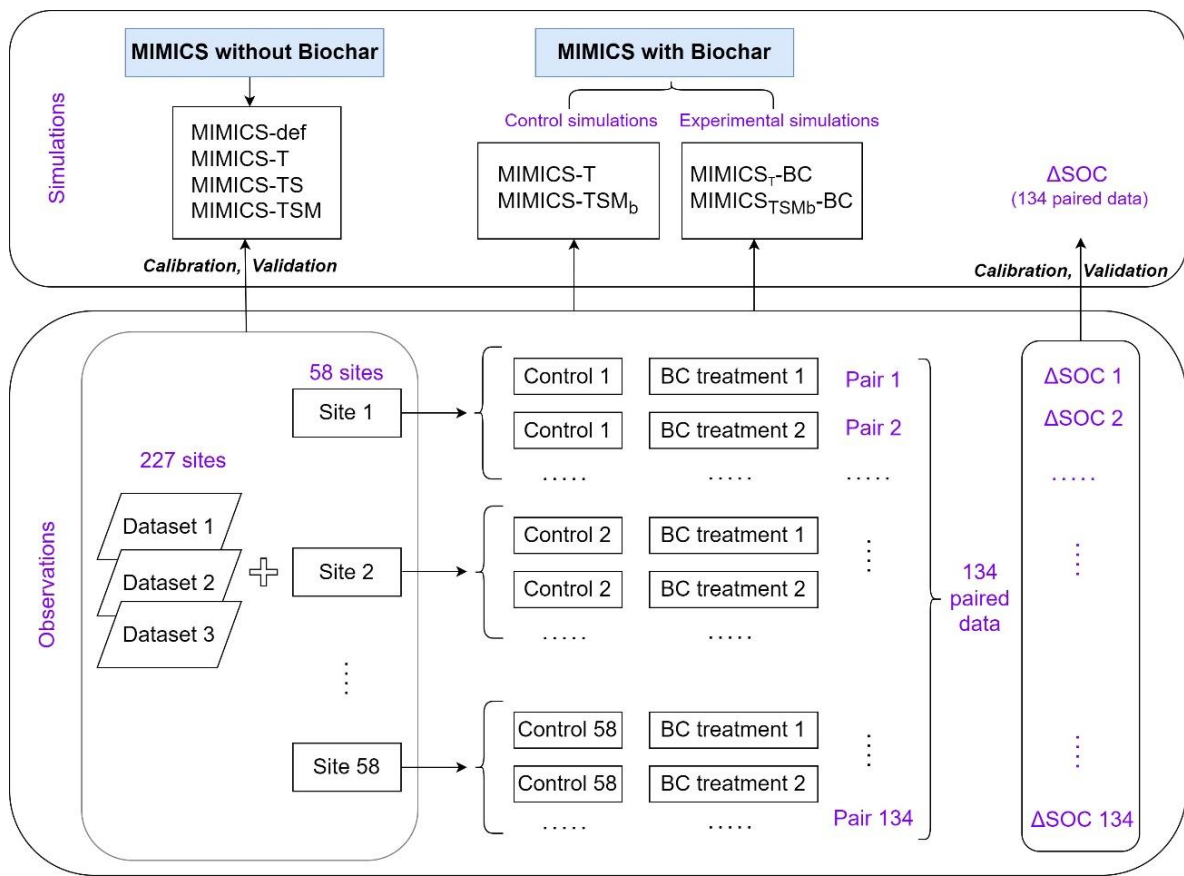
Similar to MIMICS_{T-BCDV-SOCa} but biochar is added in MIMICS-TSM_b.

Table 1 Parameters for optimization in MIMICS versions.

Datasets	Model versions	Optimized parameters	Prior value	Optimized value	Units
Cropland SOC (58 sites)	MIMICS-TSM _b	a_v	10	15.91	-
		a_k	5	13.10	-
		k_d	0.5	1.60	-
		β	1	1.47	-
		k_{ba}	6	2.95	-
		e_1	0.3	0.51	-
		e_2	3	3.86	-
Cropland SOC changes with biochar addition (134 paired data)	MIMICS-TSM _b	-	-	-	-
	MIMICS-BC _D	f_d	-0.002	-0.0038 ^a (-0.0131 ^b)	ha ⁻¹ ·C
	MIMICS-BC _{DV}	f_d	-0.002	-0.0083 ^a (-0.0095 ^b)	ha ⁻¹ ·C
		f_v	0.05	0.008 ^a (-0.0097 ^b)	ha ⁻¹ ·C

Note: a_v and a_k are the tuning coefficients for microbial maximum reaction velocity (Eq. 2) and half saturation constant (Eq. 3). k_d is the tuning coefficient for deprotection rate of SOC_p (Eq. 5). β is the density dependent microbial turnover rate (Eq. 6). k_{ba} is binding affinity (Eq. 8), and e_1 , e_2 are fitted values for estimating maximum sorption capacity of SOC_p (Eq. 9). f_d and f_v are coefficients for adjusting the deprotection rate of SOC_p (Eq. 15) and microbial decomposition velocity (Eq. 16), respectively when adding biochar. Superscripts a and b are for the optimized parameter values using the short term and long term (extended to 8 yr) SOC data, respectively.

455



460 **Fig. 3** Diagram of field measurement SOC data and the model simulation settings. The simulated or observed Δ SOC is equal to SOC with the biochar addition treatment minus that in the control treatment (without biochar addition). Note that one control treatment may correspond to multiple BC treatments with different applied BC rates at one single site.

3. Results of model calibration and validation

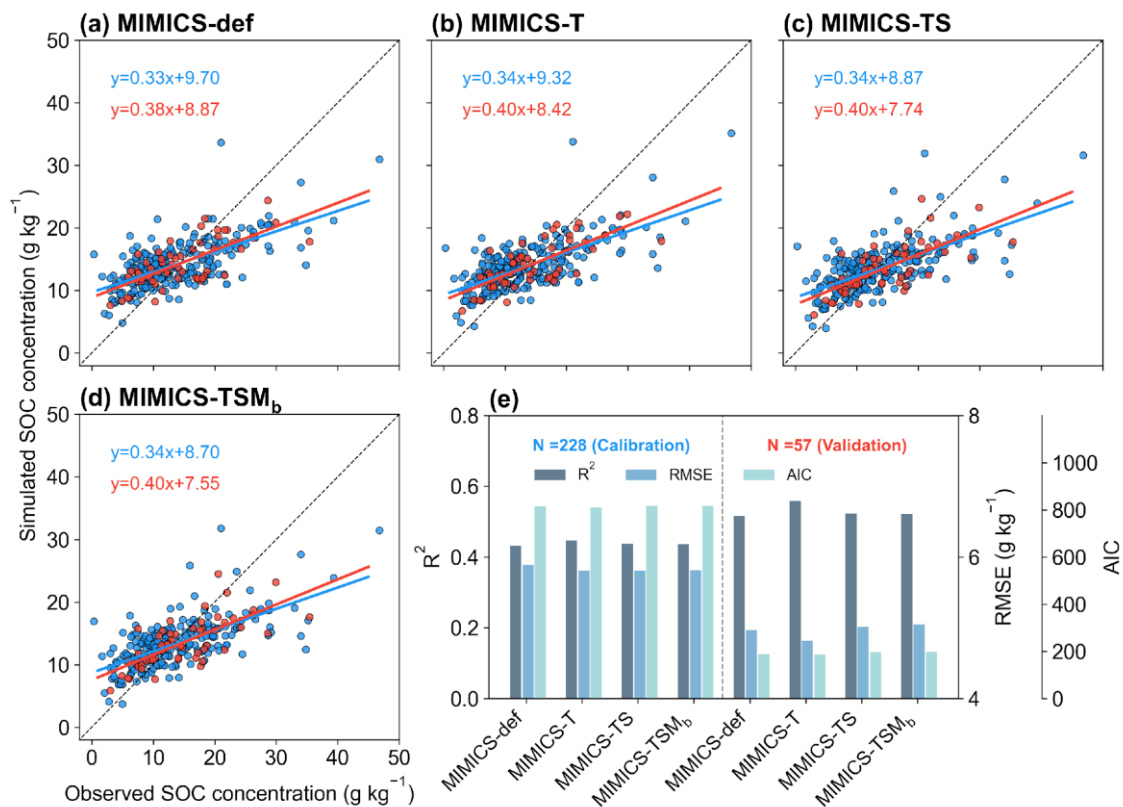
465 3.1 Performance of different MIMICS versions for simulating cropland SOC

Among the MIMICS versions without biochar optimized parameters, MIMICS-TSM_b has the highest correlation ($R^2=0.5245$; Fig. 2, Fig. S7) and the lowest RMSE (RMSE=4.41-5.81 g kg⁻¹) and lowest AIC (AIC=810.0) between the observed and simulated cropland SOC concentrations in calibration (Fig. 4, Fig. S5a). Compared to MIMICS-def ($R^2=0.3843$, RMSE=4.96-5.89 g kg⁻¹, AIC=191.88-14.8, Fig. S7S5a), all other MIMICS versions show better performances in calibration with a higher R^2 and lower RMSE of 0.47-0.52 except for MIMICS-TSM_a (Fig. S7S5a). After considering the density-dependent microbial turnover rate, MIMICS-T can better capture the observed spatial variation of SOC ($R^2=0.47$, RMSE=4.61 g kg⁻¹, AIC=185.3, Fig. 2e4, Fig. S7S5a). MIMICS-TS with alternative implementation of SOC_p adsorption explains 51.44% SOC spatial variation with a smaller RMSE (4.45-5.81 g kg⁻¹), but a larger AIC (187.28-16.6) (Fig. 2e4, Fig. S7S5a). As compared with MIMICS-TS, for the MIMICS-TSM versions that accounts for the effects of soil moisture, R^2 (0.50-0.52) does not show significantly improvement (Fig. 4, Fig. S5a). -with RMSE and AIC of 4.41-4.53 g kg⁻¹ and

475

186.0–189.2, respectively (Fig. 2; Fig. S7).

When using 20% data for the independent model evaluation, MIMICS-TS also predicted SOC performs better best with the highest accuracy ($R^2=0.38$ 56) and the lowest RMSE (4.964.82 g kg^{-1}), but and the a lowest higher AIC (52.14187.2) among all different model versions (Table S5 Fig. 4, Fig. S5). MIMICS-TS and MIMICS-TSM_b also have the better correlation ($R^2=0.52$ and 0.52), but higher RMSE (RMSE=5.01 g kg^{-1} and 5.05 g kg^{-1}) and AIC (AIC=197.7 and 198.6) between the observed and simulated cropland SOC concentration than MIMICS-def ($R^2=0.51$, RMSE=4.97 g kg^{-1} , AIC=188.8) (Fig. 4e, Fig. S7b). R² of MIMICS-TSM versions ranges from 0.46 to 0.52, and R² of MIMICS-TSM_b is highest among them. We also evaluated the performances of the different MIMICS-MIMICS-TSM_b versions using calibrate with cropland SOC data under different crop types not used in the calibration (Sun et al., 2020; Geisseler et al., 2017; Zhou et al., 2017b). MIMICS performs comparably well on these SOC datasets. R² of different MIMICS versions that were evaluated using the three SOC datasets from Sun et al. (2020), Geisseier et al. (2017) and Zhou et al. (2017b) ranges from 0.38 to 0.80, and R² of MIMICS-TSM_b is highest among all MIMICS versions (Fig. S8). The model performance varies among different cover-crop types (i.e., maize, rice and wheat). R^2 between the simulated SOC concentrations by MIMICS-TSM_b and observations is higher for maize and wheat (0.84 and 0.74, respectively, Fig. S9a, c) but lowest for rice (0.38, Fig. S9b). It is probably because the flooded condition in the paddy field limited SOC decomposition, which is partly supported by the weaker correlation between SOC and NPP for rice ($R^2=0.06$, Fig. S10d) than that for maize and wheat ($R^2=0.77$ and 0.54, Fig. S10a, S7a, g).



495 **Fig. 4** Comparison between the observed and simulated SOC concentrations by (a) MIMICS-def, (b) MIMICS-T, (c) MIMICS-TS and (d) MIMICS-TSM_b. Blue and red dots in (a-d) represent observation sites for model calibration (80% sites) and validation (20% sites). (e) R², root mean square error (RMSE) and Akaike information criterion (AIC) from the model calibration (left panel) and validation (right panel) for the four MIMICS versions. Relationships for the other MIMICS versions can be found in Fig. S8.

500 **Fig. 2** Relationships between observed and simulated SOC concentrations by various MIMICS versions at cropland sites. MIMICS-def (a) is the default model version with modified parameters related to crop properties (Section 2.2.5); MIMICS-T (b) considers the density-dependent microbial turnover rate; MIMICS-TS (c) also includes the sorption process of SOC_p; MIMICS-TSM_b (d) considers further moisture effects on SOC turnover from the ORCHIDEE-SOM model (Camino-Serrano et al., 2018). (e) R² and root mean square error (RMSE) of the four MIMICS versions. Relationships for the other MIMICS versions can be found in Fig. S11.

505

3.2 Calibration and Evaluation of the MIMICS-BC model

3.2.1 Model calibration and validation Evaluation

For the calibration of short-term SOC changes after biochar addition, MIMICS_{T-BC} and MIMICS_{TSM_b-BC} versions with new biochar processes show a better performance with higher R², lower RMSE and AIC than MIMICS-T and MIMICS-TSM_b, respectively (Fig. S9-10). For the model validation using observation data that are not used for calibration, the performance of MIMICS_{T-BC_{DV-SOC_a}} (R²=0.80, RMSE=3.38 g kg⁻¹, AIC=69.8, Fig. 5e-g) is slightly better than MIMICS_{T-BC_D} (R²=0.79, RMSE=3.43 g kg⁻¹, AIC=68.5) and MIMICS_{T-BC_{DV}} (R²=0.76, RMSE=3.66 g kg⁻¹, AIC=74.1), except for the AIC (69.8) is higher than that of MIMICS_{T-BC_D} (68.5) (Fig. 5). By comparison, the performance of MIMICS-T is poorer than these three versions. Among the MIMICS_{TSM_b-BC} versions, MIMICS_{TSM_b-BC_{DV}} performs best in reproducing SOC changes with biochar addition with the highest R² (0.79), the lowest RMSE (3.73 g kg⁻¹) and AIC (75.0) (Fig. 6e-f). We further calibrated the model at sites with a relatively longer biochar addition period of observations (Age_{BC} > 3 yr). The corresponding R² between observed and simulated SOC changes after biochar addition by MIMICS_{TSM_b-BC_{DV}} (0.20~0.67, Fig. S11c, g, k, o) are lower than that R² for all sites (0.63, Fig. S10c, e), except for sites with Age_{BC} > 3 yr (0.67, Fig. S11c).

515

For short-term SOC changes after biochar addition, the performance of MIMICS_{BC_{DV}} (R²=0.65, RMSE=3.61 g kg⁻¹, Fig. 3d, e) is slightly better than MIMICS_{TSM_b} (R²=0.63, RMSE=3.67 g kg⁻¹, Fig. 3) and MIMICS_{BC_D} (R²=0.64, RMSE=3.64 g kg⁻¹, Fig. 3d, e), but the AIC (352.57) is higher than that of MIMICS_{TSM_b} (348.57) and MIMICS_{BC_D} (350.57) (Fig. 3f). The slope of SOC changes after biochar addition between observations and simulations from MIMICS_{BC_D} (-0.77), MIMICS_{BC_{DV}} (-0.76) is also closer to 1 than the MIMICS_{TSM_b} (-0.71, Fig. 3a-c). We further evaluated the model performance at sites with a relatively longer biochar addition period of observations (Age_{BC} ≥ 3 yr). The corresponding R²

520

525 ~~between observed and simulated SOC changes after biochar addition by MIMICS-BC_{DV} (0.09–0.70, Fig. S12e, f, i, l) are lower than that R² for all sites (0.65, Fig. 3d), except for sites with Age_{BC} ≥ 3 yr (0.70, Fig. S12e).~~

For the long-term (extended to 8 yr based on biochar decomposition curve, Wang et al., 2016a) SOC changes after biochar addition, MIMICS_T-BC_{DV} and MIMICS_{TSM_b}-BC_{DV} show the best performance among all versions in the model calibration (Fig. S9-10). In the model validation, MIMICS-T and MIMICS-TSM_b underestimate the extrapolated observations of SOC change (Fig. 5a, Fig. 6a). MIMICS_T-BC_D shows the best performance with the lowest RMSE (3.84 g kg⁻¹) and AIC (74.7) among all the MIMICS_T-BC versions (Fig. 5). Compared to MIMICS-TSM_b (R²=0.88, RMSE=9.35 g kg⁻¹, slope=0.08, AIC=120.7, Fig. 6a, e, f, g), predictions of MIMICS_{TSM_b}-BC_D, MIMICS_{TSM_b}-BC_{DV} and MIMICS_{TSM_b}-BC_{DV-SOC_a} are more accurate with a smaller RMSE (8.12 g kg⁻¹, 6.08 g kg⁻¹ and 6.78 g kg⁻¹, Fig. 6f), a smaller AIC (115.1, 101.5 and 107.4, Fig. 6g), a linear slope closer to 1 (0.29, 1.68 and 1.74, Fig. 6a-d), and a reasonable accuracy of R² (0.45, 0.97 and 0.94, Fig. 6e). Among the different MIMICS_{TSM_b}-BC versions, MIMICS_{TSM_b}-BC_{DV} shows the best performance (Fig. 6). When assuming that biochar produces a priming effect only through affecting the utilization rate of SOC_a by microbes (MIMICS_{TSM_b}-BC_{DV-SOC_a}), the model accuracy is slightly decreased with lower R² (=0.94), higher RMSE (=6.78 g kg⁻¹) and higher AIC (=107.4) than MIMICS_{TSM_b}-BC_{DV} that assumes all decomposition processes were affected (Fig. 6).

540 ~~For the long term (extended to 8 yr based on biochar decomposition curve, Wang et al., 2016a) SOC changes after biochar addition, MIMICS-TSM_b underestimates the extrapolated observations of SOC change (Fig. 3a). Compared to MIMICS-TSM_b (R²=0.89, RMSE=5.62 g kg⁻¹, slope=0.38, AIC=462.76, Fig. 3a, d, e, Fig. 3f), predictions of MIMICS-BC_D and MIMICS-BC_{DV} are more accurate with a smaller RMSE (3.57 g kg⁻¹ and 3.31 g kg⁻¹, Fig. 3e), a linear slope closer to 1 (0.87 and 1.00, Fig. 3a-e), a reasonable accuracy of R² (0.83 and 0.84, Fig. 3d), but an increase in AIC (464.76 and 466.76, Fig. 3f).~~

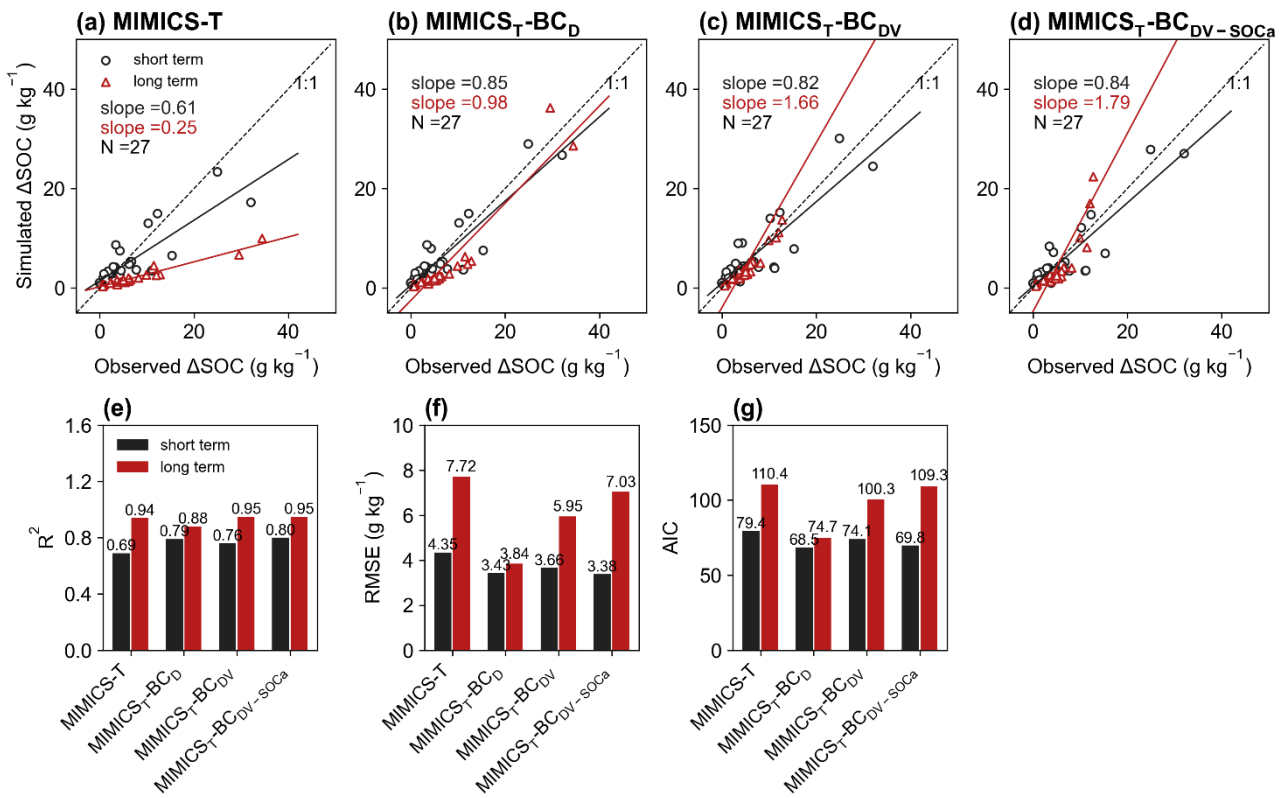
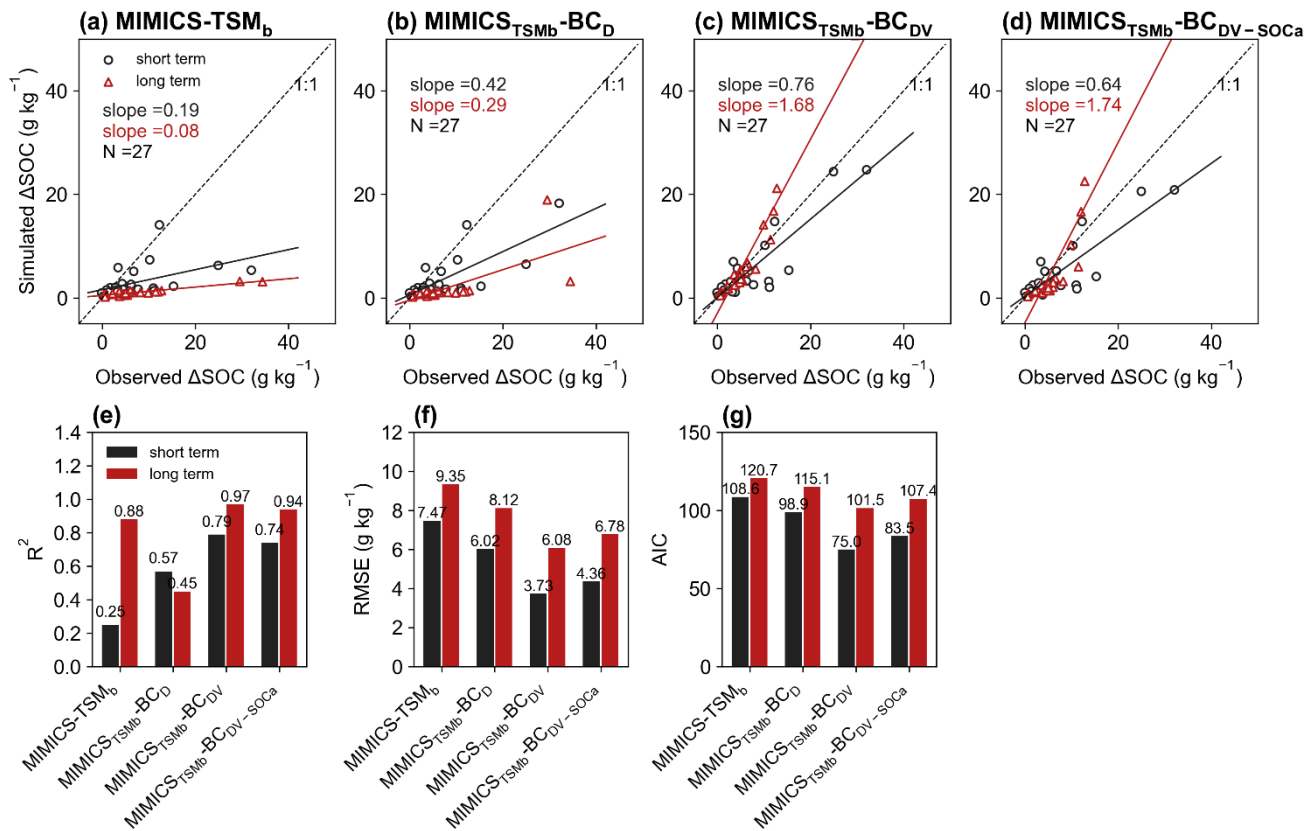


Fig. 5 Relationships of short-term (≤ 6 yr; black) and long-term (i.e., extended to 8 yr; red) SOC changes after biochar addition (Δ SOC) between observations and models in validation dataset. The MIMICS versions are used, including MIMICS-T (a), MIMICS_T-BC_D (b), MIMICS_T-BC_{DV} (c) and MIMICS_T-BC_{DV}-soCa (d). Comparisons of R² (e), the root mean square error (RMSE, f) and the Akaike information criterion (AIC, g) among the four MIMICS_T-BC versions are shown separately. See model versions in Table 1.

550



555 **Fig. 6** Relationships of short-term (≤ 6 yr; black) and long-term (i.e., extended to 8 yr; red) SOC changes after biochar addition (Δ SOC) between observations and models in validation dataset. The MIMICS versions are used, including MIMICS-TSM_b (a), MIMICS_{TSM_b}-BC_D (b), MIMICS_{TSM_b}-BC_{DV} (c) and MIMICS_{TSM_b}-BC_{DV}-SOC_a (d). Comparisons of R² (e), the root mean square error (RMSE, f) and the Akaike information criterion (AIC, g) among the four MIMICS_{TSM_b}-BC versions are shown separately. See model versions in Table 1. Relationships of short term (≤ 6 yr; pink) and long term (i.e.,

560 extended to 8 yr; light blue) SOC changes after biochar addition (Δ SOC) between observations and models. The MIMICS versions are used, including MIMICS-TSM_b (a), MIMICS-BC_D (b) and MIMICS-BC_{DV} (c). Comparisons of R² (d), the root mean square error (RMSE, e) and the Akaike information criterion (AIC, f) among the three MIMICS-BC versions are shown separately. MIMICS-TSM_b considers both the sorption process and soil moisture effects but without parameterizations for biochar addition; MIMICS-BC_D includes biochar effects on SOC by modifying deprotection rate of SOC_p in the

565 MIMICS-TSM_b (Eq. 15); MIMICS-BC_{DV} considers further biochar effects on SOC by modifying the microbial maximum reaction velocity (Eq. 16).

3.2.2 Error analysis

The biases between the simulated and observed SOC changes with biochar addition in short-term are significantly correlated ~~to~~ with Clay and MAT_Rate_BC ($p < 0.05$), but ~~and decrease~~ only marginally with SM, MAT and NPP when ~~as~~ additional

570 parameters are optimized (Fig. S13S12). For the long-term SOC changes after biochar addition, the best model version, i.e., MIMICS_{TSM_b}-BC_{DV}, can explain 84.97% of the variations of observed long-term SOC changes after biochar addition (Fig.

3e6e). The biases between long-term observations and simulations by MIMICS-TSM_b are significantly correlated to Rate_BC (r = -0.82-0.81), Age_BC (r = -0.22), Clay (r = 0.32) and BD (r = 0.20, Fig. 47), suggesting that the model may underrepresent processes related to those Rate_BC variables. By considering biochar effects on the SOC deprotection-desorption (MIMICS_{TSMb}-BC_D), the correlations of model biases with Rate_BC, Age_BC, Clay (p < 0.05), BD, SM and NPP become weaker (Fig. 47). MIMICS_{TSMb}-BC_{DV} incorporating the biochar impacts on microbial decomposition velocity further reduced reduces the correlations between model biases and variables of Rate_BC, Age_BC and BD. MIMICS_{TSMb}-BC_{DV}-SOC_a including the impacts on microbial decomposition velocity only in the flux from SOC_a to MIC pools can also reduce the correlations between model biases and variables of Rate_BC and BD, but the correlations changed little for Clay and NPP Age_BC (Fig. 7).

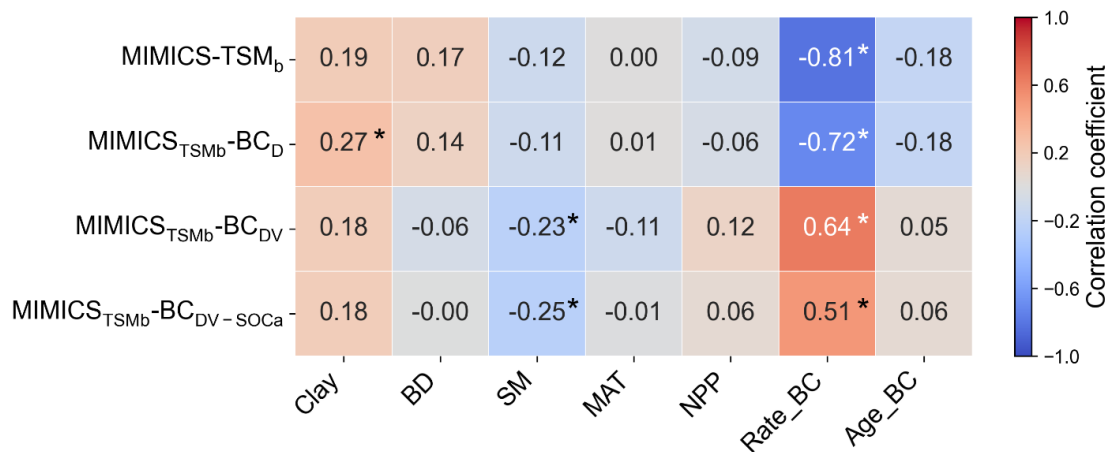


Fig. 7 Correlations between the MIMICS-BC biases (i.e., simulated long-term ΔSOC - observed ΔSOC) and input soil- (Clay, BD, SM), climate- (MAT), biological- (NPP) and biochar-related (Rate_BC, Age_BC) variables for MIMICS-TSM_b, MIMICS_{TSMb}-BC_D and MIMICS_{TSMb}-BC_{DV} and MIMICS_{TSMb}-BC_{DV}-SOC_a. Asterisks indicate significant correlations (p < 0.05).

4. Sensitivity tests and discussion

4.1 Sensitivity tests of MIMICS for simulating cropland SOC

MIMICS versions with adsorption and soil moisture effects perform well in comparison with site-level SOC concentrations on croplands collected in this study and other datasets (Fig. 24; Fig. S8S5), although the soil moisture effects are not notable. We also tried a test by assuming that soil moisture affects the microbial growth rate through mediating microbial growth (V_{max}) and turnover (τ) of MIC_r and MIC_k (Wieder et al., 2019) and thus added the soil moisture factor (i.e., $f(\theta)$ in Eq. 11) on V_{max} and τ . But the model does not predict SOC concentrations more accurately ($R^2=0.45$ - 0.46 , $RMSE=4.75$ - 0.06 g kg⁻¹, $AIC=194$ - 189.9 , Fig. S14S13b) than the MIMICS-TSM_b version where V_{max} and K_m were affected in ($R^2=0.52$, $RMSE=4.4$ - 5.05 g kg⁻¹, $AIC=186$ - 198.6 , Fig. 24d, Fig. S5b). Annual mean crop NPP, as the input of SOC pools, is also optimized within the range of

595 site-level crop NPP values similarly to other variables to test model performance in MIMICS-TSM_b, but it shows little improvement ($R^2=0.450.48$, $RMSE=4.75.12$ g kg⁻¹, $AIC=196200.2$, Fig. [S15S14b](#)), compared to MIMICS-TSM_b without NPP optimized (Fig. [244d](#)). Decomposition equations of SOC were constructed based on a wide variety of ecological assumptions, resulting in many forms (Buchkowski et al., 2017). The inverse Michaelis-Menten kinetics of soil carbon decomposition assume that the SOC decomposition rate depends nonlinearly on the enzyme concentration, but linearly on the substrate concentration (Wang et al., 2016b). We also tested MIMICS based on the inverse Michaelis-Menten kinetics in the carbon degradation processes to explore the fundamental mechanisms of SOC decomposition, but the results are similar to the forward Michael-Menten kinetics (Fig. [24](#); Fig. [S16aS15a-d](#)). In addition, we tested MIMICS for different spatial resolutions after aggregating cropland SOC sites within each 0.5° × 0.5° grid cell, and the model also performs well and can reproduce about [45%~5055%](#) of the SOC spatial variation (Fig. [S16eS15e-h](#)). [We also evaluated the response of MIMICS model to idealized warming, and the MIMICS-TSM_b version shows a slightly better performance for reproducing observed changes in soil heterotrophic respiration with warming than other versions \(Text S1\).](#)

SOC dynamics is influenced by many complex factors (e.g., pH, mineral content). In clay- or Fe-rich mineral soils, physically protected SOC might increase due to the large adsorption capacity of dissolved organic carbon onto soil mineral particles (Mayes et al., 2012). Adding the sorption process into MIMICS (MIMICS-TS) doesn't improved the model performance ($R^2=0.5144$, Fig. [2e4c](#), Fig. [S5a](#)), compared to the MIMICS-T version ($R^2=0.470.45$, Fig. [2b4b](#), Fig. [S5a](#)). In addition, management (e.g., irrigation, fertilization) are important factors that affect SOC decomposition and accumulation in croplands. The poor performance of MIMICS for rice is probably due to inability of MIMICS to simulate SOC dynamics under anaerobic condition from the irrigation practice (Fig. [S9-10S6-7](#)). Tillage may disrupt soil aggregates and release physically protected SOC, which is more susceptible to decomposition than that protected by soil aggregates (Six et al., 1999). Juice et al. (2022) modeled tillage effects on SOC loss through transferring protected SOC into unprotected pools, i.e., from SOC_p to SOC_a in this study. Although lacking sufficient tillage information at the sites we studies here, we attempted to include tillage disturbance effects in MIMICS by assuming a fixed 30% increase of ~~deprotection~~[desorption](#) rate of SOC_p according to Juice et al. (2022) (i.e., $D \times (1+30\%)$, Eq. 5), but R^2 between observations and simulations ($0.46\sim0.510.57$, Fig. [S16iS15i-l](#)) is similar to that from the version without tillage ($R^2 = 0.470.51\sim0.520.56$, Fig. [24](#), Fig. [S5b](#)). [By considering more plausible mechanisms, the performance of MIMICS model changes little with a slightly higher AIC. It is possible that the model is still not fully constrained. With more emerging technologies and observation data available, the parameters related to these processes can be further calibrated.](#)

625 In addition, cropland management disturbs soils frequently, and the assumed equilibrium state of SOC may not be realistic, which also partly explains the mismatch between simulated and observed SOC. We thus added sensitivity tests by perturbing

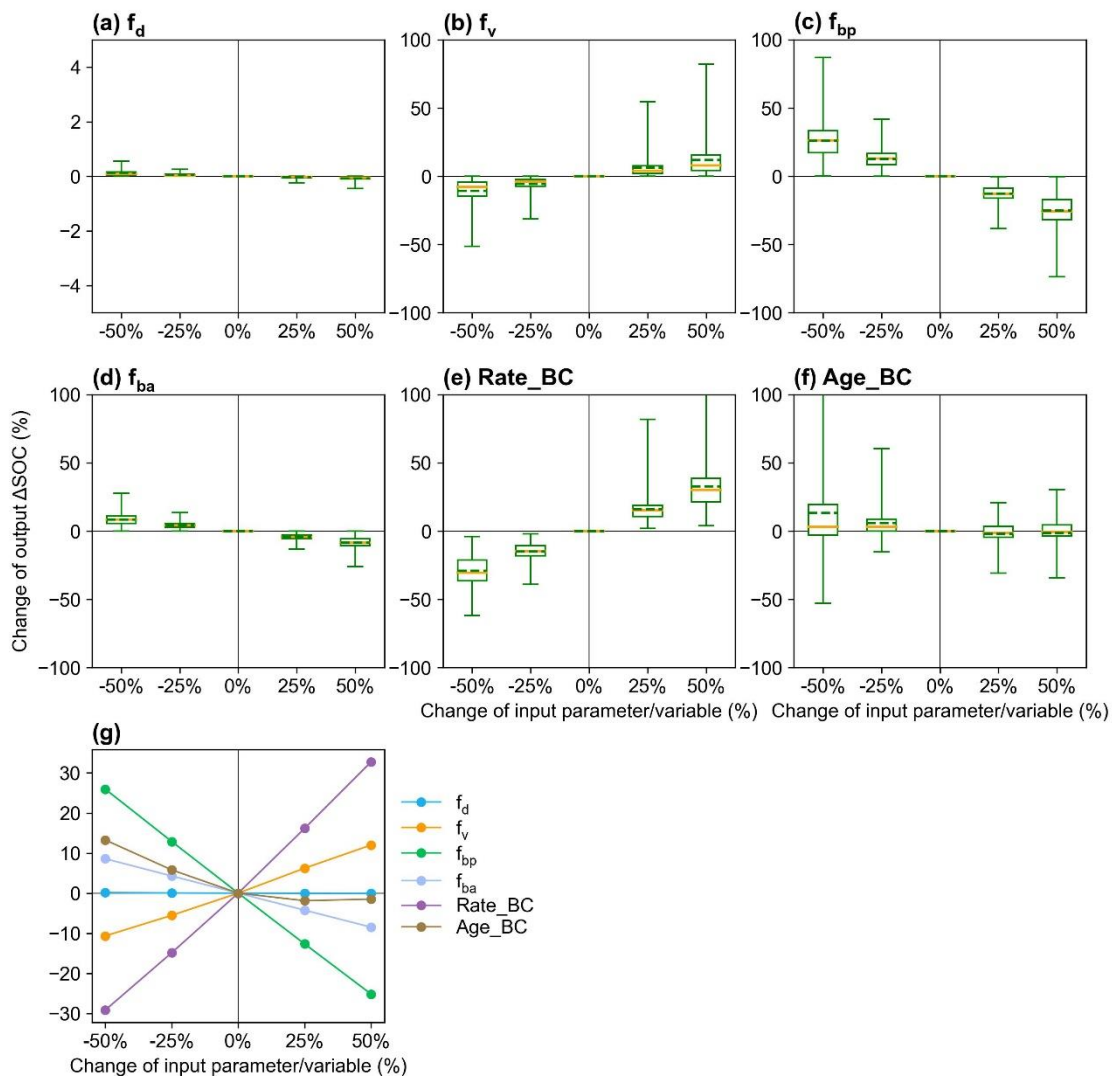
the input variables (MAT, Clay, NPP, SM and BD) to evaluate the steady SOC changes and the possible impacts of non-steady states on the results. The size of SOC pool is positively correlated with NPP and Clay, but negatively correlated with MAT and BD. The responses of steady SOC to the perturbation of BD, MAT and NPP are relatively large (Fig. S17S16), indicating that processes related to these variables have a great effect on the steady SOC. The soil BD was found to be affected by tillage practices (Osunbitan et al., 2005), and crop NPP may vary due to crop rotation, fallow or fertilization. Therefore, agricultural management practices, such as fertilization and crop rotation, need to be incorporated in soil carbon models in future to reduce the uncertainty of simulating cropland SOC dynamics (Campbell et al., 2007; Congreves et al., 2015).

4.2 Sensitivity tests and uncertainty for MIMICS-BC

The MIMICS-BC versions have a good performance in reproducing the observed short-term SOC changes with biochar addition ($R^2 = 0.63-0.65-0.57-0.79$ for MIMICS_{TSM_b}-BC versions, Fig. 36). It is probably due to the high correlation between Rate_BC and Δ SOC ($r = 0.74-0.71$, Fig. S13S12), indicating that the biochar application rate dominates changes in SOC concentrations over a short period. For the long-term changes (extended to 8 yr), MIMICS_{TSM_b}-BC versions show a greater improvement than the MIMICS-TSM_b version (Fig. 36). Biochar can absorb SOC due to its large specific surface area, high porosity and further promotion of soil macro-aggregates formation (Han et al., 2020; Huang et al., 2018). Consistently, the optimized ~~deprotection~~desorption coefficient ($f_d = -0.0038-0.0121$ and $-0.0131-0.0122$ for short- and long-term, Table S3) in MIMICS-BC_D is negative, indicating the carbon ~~deprotection~~desorption from SOC_p to SOC_a is reduced with biochar addition, ~~and the biochar effect on SOC sorption/desorption over long term is stronger than that in short term~~. Incorporating the biochar impacts on microbial decomposition velocity in the MIMICS_{TSM_b}-BC_{DV} further improved model with biochar addition in long term (decomposition rate coefficient (f_v) = $-0.0097-0.0253$, Table S3). ~~The correlations between model-observation biases and input variables become weaker for MIMICS-BC_{DV}, but the correlation with clay is still significant ($p < 0.05$, Fig. 7), implying that some processes related to the variable are not well represented in the model.~~ ~~MIMICS-BC_{DV} further reduced the correlations between model-observation biases and input variables, but the correlation with Clay is still significant ($p < 0.05$, Fig. 4), implying that some processes related to the variable are not well represented in the model.~~ The responses of Δ SOC to parameter perturbations show that f_v and f_d affect Δ SOC changes with biochar addition in opposite directions, and Δ SOC is more sensitive to the partition coefficient from biochar carbon to SOC_p (f_{bp}) than f_d, f_v and the partition coefficient from biochar carbon to SOC_a (f_{ba}) (Fig. S8). Among the input variables, Δ SOC is more sensitive to Rate_BC than Age_BC.

Biochar stability, which could affect priming effects, varies with biochar feedstock types and pyrolysis temperature (Wang et al., 2016a). Using wood and straw as biochar feedstock, 0.3% and 0.8% of biochar carbon is lost at a pyrolysis temperature of 800 °C (wood) and 350 °C (straw), respectively (Hamer et al., 2004). 2% of biochar carbon was assumed to distribute into active/metabolic pool in the EPIC model (The Environmental Policy Integrated Climate, Lychuk et al., 2014), and thus we

660 tested the MIMICS_{TSMb}-BC model with the partition coefficient from biochar carbon to SOC_a (f_{ba}) = 2%, and the model shows a lower-similar R^2 (0.60.35~0.79, Fig. S18S17) than-to that f_{ba} = 20% in short-term (0.650.25~0.79, Fig. 36). We further optimized the partition coefficient from biochar carbon to SOC_p (f_{bp}) and f_{ba} based on MIMICS_{TSMb}-BC_{DV} to test the parameter uncertainties. The optimized version (MIMICS_{TSMb}-BC_{DV}*) shows a better performance (R^2 =0.670.80, RMSE=3.63.44 g kg⁻¹, AIC=35066.7, Fig. S19S18) than MIMICS_{TSMb}-BC_{DV}, and the optimized f_{bp} , f_{ba} and the partition coefficient from biochar carbon to SOC_c (f_{bc}) are 59.658.1%, 29.18.2% and 44.333.7%, respectively. Compared to MIMICS_{TSMb}-BC_{DV}, Correlations correlations of MIMICS_{TSMb}-BC_{DV}* model errors with Clay, BD, SM and NPP reduced, but the correlations with Rate_BC and BD-Age_BC increased (Fig. S13S12). We also added a test to evaluate the performance of the MIMICS-BC versions in simulating the changes of SOC, MIC and soil respiration fluxes after biochar addition in our collected paired sites. Results show that MIMICS_{TSMb}-BC_{DV} and MIMICS_{TSMb}-BC_{DV}-SOC_a are the better versions for reproducing the observed changes in SOC, MIC and respiration among the four MIMICS_{TSMb}-BC versions (Text S2).



670 **Fig. 8** Sensitivity analysis of MIMICS-BC model parameters of (a) f_d (deprotection-desorption coefficient, Eq. 15), (b) f_v (decomposition rate coefficient, Eq. 16), (c) f_{bp} (partition coefficient from biochar carbon to SOC_p, Fig. 1), (d) f_{ba} (partition

coefficient from biochar carbon to SOC_a, Fig. 1), and the biochar-related input variables, (e) Rate_BC and (f) Age_BC. The yellow line and green dotted line in boxplots are median and mean values of the changes in model output (i.e., change of ΔSOC, Eq. 19). The mean values of change of output ΔSOC in all sites are shown in (g).

675

The effects of biochar on SOC are controlled by various factors, such as soil physicochemical and biological properties (e.g., clay, pH, microbial activity), biochar properties (e.g., feedstock, pyrolysis temperature) and incubation conditions (e.g., periods, ~~cover~~-crop types) (Ding et al., 2017; Han et al., 2020). Some of these effects are not explicitly considered in the MIMICS biochar version. Microbial carbon use efficiency (CUE) determines the relation proportions of microbial carbon uptake between growth and respiration (Zhou et al., 2017a), and increased CUE and reduced turnover time ($1/\tau$) of microbial biomass were found with biochar addition, although the changes depend on the soil texture (Pei et al., 2021). We conducted additional sensitivity tests with assumed perturbation levels in these parameters (MGE and τ) and input variables (NPP, Clay and SM) in the simulations with biochar addition. MGE and τ are very important parameters to the model outputs, while the impacts of NPP, Clay and SM are relatively small (Fig. [S20S19](#)). Therefore, processes and parameters related to MGE and τ need to be accounted for in future with more evidence.

685

Biochar addition may also change the composition of microbial community, and a previous study reported increased copiotrophic bacteria with a higher growth rate and decreased oligotrophic bacteria in acid soils with biochar addition (Sheng & Zhu, 2018). This is related to the competition between r- and k-strategy microbes in MIMICS. In the MIMICS-BC version, we assumed that biochar, with a longer turnover time (about 1000 yr, Schmidt et al., 2002) than SOC, are evenly mixed with SOC and are treated as a homogenous pool without an explicit vertical profile, which may also bring uncertainties. In addition, due to lack of long-term biochar addition experiments, the extended long-term SOC concentrations with biochar addition is calculated as the sum of SOC in the control site without biochar addition and the remaining biochar carbon based on the biochar degradation curve (Fig. [S6S4](#); Wang et al., 2016a). Although they are not direct observations and may induce uncertainty, the long-term model validation is important to assess the model ability of simulating the SOC stability with biochar addition. Long-term and comprehensive field measurements of SOC and other soil and microbe properties after biochar addition are therefore urgently needed to understand the underlying mechanisms of biochar impacts on SOC changes, all of which will help improve the model performance.

695

5. Conclusion

~~In this study, we developed several updated MIMICS versions with new processes (e.g., adsorption and soil moisture) and attempted to incorporate biochar into MIMICS to simulate the effects of biochar on SOC dynamics. We further validated MIMICS against field measurements on global croplands without and with biochar addition. However, management practices~~

700

such as tillage, fertilization and irrigation on croplands are intensive, raising challenges in representing these processes in the soil carbon models due to lack of spatially explicit input data and poor understanding of the mechanisms. Therefore, more long term field experiments for biochar addition will help better represent biochar processes in the soil carbon model and evaluate the model performance. Biochar is believed to have a large CDR potential, and its application on soils would affect the soil carbon and nutrient cycles. These impacts need to be incorporated ESMs to accurately simulate the mitigation potential of biochar under future climate change.

Our study shows that the updated MIMICS versions with new processes (e.g., adsorption and soil moisture) improves the model performance on simulating SOC dynamics on croplands. The model versions implemented with biochar processes can generally capture the SOC changes after biochar application from observations. Biochar is believed to have a large CDR potential, and its application on soils would affect the soil carbon and nutrient cycles. These impacts need to be incorporated ESMs to accurately simulate the mitigation potential of biochar under future climate change.

715 Code availability. The codes of this model version are available at <https://doi.org/10.5281/zenodo.8112967> (Han et al., 2023).

Author contributions. Mengjie Han collected the site measurements data for model evaluation, performed the simulations and optimized the model code, and prepared the manuscript. Qing Zhao and Wei Li conceived the study and designed the experiments. Wei Li, Ying-Ping Wang, Philippe Ciais, Haicheng Zhang, Daniel S. Goll, Chen Wang and Wei Zhuang guided and improved the manuscript in technology, logic and detail. Lei Zhu, Zhe Zhao and Zhixuan Guo assisted with the technical aspects in data acquisition and analysis. Xili Wang and Fengchang Wu reviewed and revised the manuscript.

Competing interests. The authors declare that they have no conflict of interest.

725 Acknowledgements. This study was funded by the Yunnan Major Scientific and Technological Projects (grant number: CB23258N002A), the National Natural Science Foundation of China (grant number: 42192574, 42022056, 42175169) and Tsinghua University Initiative Scientific Research Program (grant number: 20223080041).

730

735 **References**

- Abiven, S., Recous, S., Reyes, V., & Oliver, R.: Mineralisation of C and N from root, stem and leaf residues in soil and role of their biochemical quality, *Biology and Fertility of Soils*, *42*, 119-128, doi:10.1007/s00374-005-0006-0, 2005.
- Abramoff, R. Z., Guenet, B., Zhang, H., Georgiou, K., Xu, X., Rossel, R. A. V., Yuan, W., and Ciais, P.: Improved global-scale predictions of soil carbon stocks with Millennial Version 2, *Soil Biology and Biochemistry*, *164*, 108466, 2022.
- 740 Akaike, H.: A new look at the statistical model identification, *IEEE transactions on automatic control*, *19*, 716-723. 1974.
- Allison, S. D., Wallenstein, M. D., & Bradford, M. A.: Soil-carbon response to warming dependent on microbial physiology, *Nature Geoscience*, *3*, 336-340, doi:10.1038/ngeo846, 2010.
- Archontoulis, S. V., Huber, I., Miguez, F. E., Thorburn, P. J., Rogovska, N., & Laird, D. A.: A model for mechanistic and system assessments of biochar effects on soils and crops and trade-offs, *GCB Bioenergy*, *8*, 1028-1045, doi:10.1111/gcbb.12314, 2016.
- 745 Bond-Lamberty, B., Bailey, V. L., Chen, M., Gough, C. M., & Vargas, R.: Globally rising soil heterotrophic respiration over recent decades, *Nature*, *560*, 80-83, doi:10.1038/s41586-018-0358-x, 2018.
- Buchkowski, R. W., Bradford, M. A., Grandy, A. S., Schmitz, O. J., & Wieder, W. R.: Applying population and community ecology theory to advance understanding of belowground biogeochemistry, *Ecol Lett*, *20*, 231-245, doi:10.1111/ele.12712, 2017.
- 750 Camino-Serrano, M., Guenet, B., Luysaert, S., Ciais, P., Bastrikov, V., De Vos, B., Gielen, B., Gleixner, G., Jornet-Puig, A., Kaiser, K., Kothawala, D., Lauerwald, R., Peñuelas, J., Schrumpf, M., Vicca, S., Vuichard, N., Walmsley, D., & Janssens, I. A.: ORCHIDEE-SOM: modeling soil organic carbon (SOC) and dissolved organic carbon (DOC) dynamics along vertical soil profiles in Europe, *Geoscientific Model Development*, *11*, 937-957, doi:10.5194/gmd-11-937-2018, 2018.
- 755 Campbell, C. A., VandenBygaart, A. J., Zentner, R. P., McConkey, B. G., Smith, W., Lemke, R., Grant, B., & Jefferson, P. G.: Quantifying carbon sequestration in a minimum tillage crop rotation study in semiarid southwestern Saskatchewan, *Canadian Journal of Soil Science*, *87*, 235-250, doi:10.4141/s06-018, 2007.
- 760 Congreves, K. A., Grant, B. B., Campbell, C. A., Smith, W. N., VandenBygaart, A. J., Kröbel, R., Lemke, R. L., & Desjardins, R. L.: Measuring and Modeling the Long-Term Impact of Crop Management on Soil Carbon Sequestration in the Semiarid Canadian Prairies, *Agronomy Journal*, *107*, 1141-1154, doi:10.2134/agronj15.0009, 2015.
- Ding, F., Van Zwieten, L., Zhang, W., Weng, Z., Shi, S., Wang, J., & Meng, J.: A meta-analysis and critical evaluation of influencing factors on soil carbon priming following biochar amendment, *Journal of Soils and Sediments*, *18*, 1507-1517, doi:10.1007/s11368-017-1899-6, 2017.
- 765 Duan, Q. Y., Sorooshian, S., & Gupta, V. K.: Optimal use of the SCE-UA global optimization method for calibrating watershed models, *Journal of Hydrology*, *158*, 265-284, doi:10.1016/0022-1694(94)90057-4, 1994.
- Eglin, T., Ciais, P., Piao, S. L., Barre, P., Bellassen, V., Cadule, P., Chenu, C., Gasser, T., Koven, C., Reichstein, M., & Smith, P.: Historical and future perspectives of global soil carbon response to climate and land-use changes, *Tellus B: Chemical and Physical Meteorology*, *62*, 700-718, doi:10.1111/j.1600-0889.2010.00499.x, 2010.
- 770 El-Naggar, A., El-Naggar, A. H., Shaheen, S. M., Sarkar, B., Chang, S. X., Tsang, D. C. W., Rinklebe, J., & Ok, Y. S.: Biochar composition-dependent impacts on soil nutrient release, carbon mineralization, and potential environmental risk: A review, *J Environ Manage*, *241*, 458-467, doi:10.1016/j.jenvman.2019.02.044, 2019.
- 775 Entekhabi, D., Njoku, E. G., O'Neill, P. E., Kellogg, K. H., Crow, W. T., Edelstein, W. N., Entin, J. K., Goodman, S. D., Jackson, T. J., Johnson, J., Kimball, J., Piepmeier, J. R., Koster, R. D., Martin, N., McDonald, K. C., Moghaddam, M., Moran, S., Reichle, R., Shi, J. C., Spencer, M. W., Thurman, S. W., Tsang, L., & Van Zyl, J.: The Soil Moisture Active Passive (SMAP) Mission, *Proceedings of the IEEE*, *98*, 704-716, doi:10.1109/jproc.2010.2043918, 2010.
- Fick, S. E., & Hijmans, R. J.: WorldClim 2: new 1-km spatial resolution climate surfaces for global land areas, *International Journal of Climatology*, *37*, 4302-4315, doi:10.1002/joc.5086, 2017.
- 780 Fuss, S., Lamb, W. F., Callaghan, M. W., Hilaire, J., Creutzig, F., Amann, T., Beringer, T., de Oliveira Garcia, W., Hartmann,

- J., Khanna, T., Luderer, G., Nemet, G. F., Rogelj, J., Smith, P., Vicente, J. L. V., Wilcox, J., del Mar Zamora Dominguez, M., & Minx, J. C.: Negative emissions—Part 2: Costs, potentials and side effects, *Environmental Research Letters*, 13, doi:10.1088/1748-9326/aabf9f, 2018.
- 785 Geisseler, D., Linqvist, B. A., & Lazicki, P. A.: Effect of fertilization on soil microorganisms in paddy rice systems – A meta-analysis, *Soil Biology and Biochemistry*, 115, 452-460, doi:10.1016/j.soilbio.2017.09.018, 2017.
- Georgiou, K., Abramoff, R. Z., Harte, J., Riley, W. J., & Torn, M. S.: Microbial community-level regulation explains soil carbon responses to long-term litter manipulations, *Nat Commun*, 8, 1223, doi:10.1038/s41467-017-01116-z, 2017.
- Hamer, U., Marschner, B., Brodowski, S., & Amelung, W.: Interactive priming of black carbon and glucose mineralisation, *Organic Geochemistry*, 35, 823-830. 2004.
- 790 Han, L., Sun, K., Yang, Y., Xia, X., Li, F., Yang, Z., & Xing, B.: Biochar's stability and effect on the content, composition and turnover of soil organic carbon, *Geoderma*, 364, doi:10.1016/j.geoderma.2020.114184, 2020.
- Han, M., Zhao, Q., Li, W., Ciais, P., Wang, Y. P., Goll, D. S., Zhu, L., Zhao, Z., Wang, J., Wei, Y., & Wu, F.: Global soil organic carbon changes and economic revenues with biochar application, *GCB Bioenergy*, 14, 364-377, doi:10.1111/gcbb.12915, 2021.
- 795 Harris, I., Jones, P. D., Osborn, T. J., & Lister, D. H.: Updated high-resolution grids of monthly climatic observations - the CRU TS3.10 Dataset, *International Journal of Climatology*, 34, 623-642, doi:10.1002/joc.3711, 2014.
- Hicke, J. A., & Lobell, D. B.: Spatiotemporal patterns of cropland area and net primary production in the central United States estimated from USDA agricultural information, *Geophysical Research Letters*, 31. 2004.
- 800 Houska, T., Kraft, P., Chamorro-Chavez, A., & Breuer, L.: SPOTting Model Parameters Using a Ready-Made Python Package, *PLoS One*, 10, e0145180, doi:10.1371/journal.pone.0145180, 2015.
- Huang, R., Tian, D., Liu, J., Lv, S., He, X., & Gao, M.: Responses of soil carbon pool and soil aggregates associated organic carbon to straw and straw-derived biochar addition in a dryland cropping mesocosm system, *Agriculture, Ecosystems & Environment*, 265, 576-586, doi:10.1016/j.agee.2018.07.013, 2018.
- 805 [Jansson, J. K. and Wu, R.: Soil viral diversity, ecology and climate change, *Nature Reviews Microbiology*, 21, 296-311, 10.1038/s41579-022-00811-z, 2023.](https://doi.org/10.1038/s41579-022-00811-z)
- Juice, S. M., Walter, C. A., Allen, K. E., Berardi, D. M., Hudiburg, T. W., Sulman, B. N., & Brzostek, E. R.: A new bioenergy model that simulates the impacts of plant-microbial interactions, soil carbon protection, and mechanistic tillage on soil carbon cycling, *GCB Bioenergy*, 14, 346-363, doi:10.1111/gcbb.12914, 2022.
- 810 Kalbitz, K., Schwesig, D., Rethemeyer, J., & Matzner, E.: Stabilization of dissolved organic matter by sorption to the mineral soil, *Soil Biology and Biochemistry*, 37, 1319-1331, doi:10.1016/j.soilbio.2004.11.028, 2005.
- Kobayashi, S., Ota, Y., Harada, Y., Ebita, A., Moriya, M., Onoda, H., Onogi, K., Kamahori, H., Kobayashi, C., Endo, H., Miyaoka, K., & Takahashi, K.: The JRA-55 Reanalysis: General Specifications and Basic Characteristics, *Journal of the Meteorological Society of Japan. Ser. II*, 93, 5-48, doi:10.2151/jmsj.2015-001, 2015.
- 815 Lehmann, J., Cowie, A., Masiello, C. A., Kammann, C., Woolf, D., Amonette, J. E., Cayuela, M. L., Camps-Arbestain, M., & Whitman, T.: Biochar in climate change mitigation, *Nature Geoscience*, 14, 883-892, doi:10.1038/s41561-021-00852-8, 2021.
- Li, Z., Song, Z., Singh, B. P., & Wang, H.: The impact of crop residue biochars on silicon and nutrient cycles in croplands, *Sci Total Environ*, 659, 673-680, doi:10.1016/j.scitotenv.2018.12.381, 2019.
- 820 [Liang, J., Wang, G., Ricciuto, D. M., Gu, L., Hanson, P. J., Wood, J. D., and Mayes, M. A.: Evaluating the E3SM land model version 0 \(ELMv0\) at a temperate forest site using flux and soil water measurements, *Geoscientific Model Development*, 12, 1601-1612, 10.5194/gmd-12-1601-2019, 2019.](https://doi.org/10.5194/gmd-12-1601-2019)
- Luo, Y., Durenkamp, M., De Nobili, M., Lin, Q., & Brookes, P. C.: Short term soil priming effects and the mineralisation of biochar following its incorporation to soils of different pH, *Soil Biology and Biochemistry*, 43, 2304-2314, doi:10.1016/j.soilbio.2011.07.020, 2011.
- 825 Luo, Y., Zang, H., Yu, Z., Chen, Z., Gunina, A., Kuzyakov, Y., Xu, J., Zhang, K., & Brookes, P. C.: Priming effects in biochar enriched soils using a three-source-partitioning approach: 14C labelling and 13C natural abundance, *Soil Biology and Biochemistry*, 106, 28-35. 2017.

- Lychuk, T. E., Izaurrealde, R. C., Hill, R. L., McGill, W. B., & Williams, J. R.: Biochar as a global change adaptation: predicting biochar impacts on crop productivity and soil quality for a tropical soil with the Environmental Policy Integrated Climate (EPIC) model, *Mitigation and Adaptation Strategies for Global Change*, 20, 1437-1458, doi:10.1007/s11027-014-9554-7, 2014.
- Manzoni, S., & Porporato, A.: Soil carbon and nitrogen mineralization: Theory and models across scales, *Soil Biology and Biochemistry*, 41, 1355-1379, doi:10.1016/j.soilbio.2009.02.031, 2009.
- Manzoni, S., Schimel, J. P., & Porporato, A.: Responses of soil microbial communities to water stress: results from a meta-analysis, *Ecology*, 93, 930-938, doi:10.1890/11-0026.1, 2012.
- Mayes, M. A., Heal, K. R., Brandt, C. C., Phillips, J. R., & Jardine, P. M.: Relation between Soil Order and Sorption of Dissolved Organic Carbon in Temperate Subsoils, *Soil Science Society of America Journal*, 76, 1027-1037, doi:10.2136/sssaj2011.0340, 2012.
- Minasny, B., Malone, B. P., McBratney, A. B., Angers, D. A., Arrouays, D., Chambers, A., Chaplot, V., Chen, Z.-S., Cheng, K., Das, B. S., Field, D. J., Gimona, A., Hedley, C. B., Hong, S. Y., Mandal, B., Marchant, B. P., Martin, M., McConkey, B. G., Mulder, V. L., O'Rourke, S., Richer-de-Forges, A. C., Odeh, I., Padarian, J., Paustian, K., Pan, G., Poggio, L., Savin, I., Stolbovov, V., Stockmann, U., Sulaeman, Y., Tsui, C.-C., Vågen, T.-G., van Wesemael, B., & Winowiecki, L.: Soil carbon 4 per mille, *Geoderma*, 292, 59-86, doi:10.1016/j.geoderma.2017.01.002, 2017.
- Minx, J. C., Lamb, W. F., Callaghan, M. W., Fuss, S., Hilaire, J., Creutzig, F., Amann, T., Beringer, T., de Oliveira Garcia, W., Hartmann, J., Khanna, T., Lenzi, D., Luderer, G., Nemet, G. F., Rogelj, J., Smith, P., Vicente Vicente, J. L., Wilcox, J., & del Mar Zamora Dominguez, M.: Negative emissions—Part 1: Research landscape and synthesis, *Environmental Research Letters*, 13, doi:10.1088/1748-9326/aabf9b, 2018.
- Moyano, F. E., Manzoni, S., & Chenu, C.: Responses of soil heterotrophic respiration to moisture availability: An exploration of processes and models, *Soil Biology and Biochemistry*, 59, 72-85, doi:10.1016/j.soilbio.2013.01.002, 2013.
- Muttill, N., & Jayawardena, A. W.: Shuffled Complex Evolution model calibrating algorithm: enhancing its robustness and efficiency, *Hydrological Processes*, 22, 4628-4638, doi:10.1002/hyp.7082, 2008.
- Omondi, M. O., Xia, X., Nahayo, A., Liu, X., Korai, P. K., & Pan, G.: Quantification of biochar effects on soil hydrological properties using meta-analysis of literature data, *Geoderma*, 274, 28-34, doi:10.1016/j.geoderma.2016.03.029, 2016.
- Osunbitan, J., Oyedele, D., & Adekalu, K.: Tillage effects on bulk density, hydraulic conductivity and strength of a loamy sand soil in southwestern Nigeria, *Soil and Tillage Research*, 82, 57-64. 2005.
- Palansooriya, K. N., Wong, J. T. F., Hashimoto, Y., Huang, L., Rinklebe, J., Chang, S. X., Bolan, N., Wang, H., & Ok, Y. S.: Response of microbial communities to biochar-amended soils: a critical review, *Biochar*, 1, 3-22, doi:10.1007/s42773-019-00009-2, 2019.
- Parton, W. J., Morgan, J. A., Kelly, R. H., & Ojima, D.: Modeling soil C responses to environmental change in grassland systems[M] The potential of US grazing lands to sequester carbon and mitigate the greenhouse effect. 2000.
- Pei, J., Li, J., Mia, S., Singh, B., Wu, J., & Dijkstra, F. A.: Biochar aging increased microbial carbon use efficiency but decreased biomass turnover time, *Geoderma*, 382, doi:10.1016/j.geoderma.2020.114710, 2021.
- [Press WH, Teukolsky SA, Vetterling WT and Flannery BP.: Numerical Recipes. The arts of Scientific Computing \(3rd edition\). New York, Cambridge University Press, 2007.](#)
- Roberts, K. G., Gloy, B. A., Joseph, S., Scott, N. R., & Lehmann, J.: Life Cycle Assessment of Biochar Systems: Estimating the Energetic, Economic, and Climate Change Potential, *Environmental Science & Technology*, 44, 827-833, doi:10.1021/es902266r, 2010.
- Schimel, J., Balsler, T. C., & Wallenstein, M.: Microbial stress-response physiology and its implications for ecosystem function, *Ecology*, 88, 1386-1394, doi:10.1890/06-0219, 2007.
- Schimel, J. P., & Weintraub, M. N.: The implications of exoenzyme activity on microbial carbon and nitrogen limitation in soil: a theoretical model, *Soil Biology and Biochemistry*, 35, 549-563. 2003.
- Schmidt, M. W., Skjemstad, J. O., & Jäger, C.: Carbon isotope geochemistry and nanomorphology of soil black carbon:

- Black chernozemic soils in central Europe originate from ancient biomass burning, *Global Biogeochemical Cycles*, *16*, 70-71-70-78. 2002.
- Shangguan, W., Dai, Y., Duan, Q., Liu, B., & Yuan, H.: A global soil data set for earth system modeling, *Journal of Advances in Modeling Earth Systems*, *6*, 249-263, doi:10.1002/2013ms000293, 2014.
- 880 Sheng, Y., & Zhu, L.: Biochar alters microbial community and carbon sequestration potential across different soil pH, *Sci Total Environ*, *622-623*, 1391-1399, doi:10.1016/j.scitotenv.2017.11.337, 2018.
- Singh, B. P., & Cowie, A. L.: Long-term influence of biochar on native organic carbon mineralisation in a low-carbon clayey soil, *Scientific reports*, *4*, 1-9. 2014.
- Six, J., Elliott, E., & Paustian, K.: Aggregate and soil organic matter dynamics under conventional and no-tillage systems, *Soil Science Society of America Journal*, *63*, 1350-1358. 1999.
- 885 Smith, P.: Soil carbon sequestration and biochar as negative emission technologies, *Glob Chang Biol*, *22*, 1315-1324, doi:10.1111/gcb.13178, 2016.
- Song, G., Li, L., Pan, G., & Zhang, Q.: Topsoil organic carbon storage of China and its loss by cultivation, *Biogeochemistry*, *74*, 47-62, doi:10.1007/s10533-004-2222-3, 2005.
- 890 Sulman, B. N., Moore, J. A. M., Abramoff, R., Averill, C., Kivlin, S., Georgiou, K., Sridhar, B., Hartman, M. D., Wang, G., Wieder, W. R., Bradford, M. A., Luo, Y., Mayes, M. A., Morrison, E., Riley, W. J., Salazar, A., Schimel, J. P., Tang, J., & Classen, A. T.: Multiple models and experiments underscore large uncertainty in soil carbon dynamics, *Biogeochemistry*, *141*, 109-123, doi:10.1007/s10533-018-0509-z, 2018.
- Sun, W., Canadell, J. G., Yu, L., Yu, L., Zhang, W., Smith, P., Fischer, T., & Huang, Y.: Climate drives global soil carbon sequestration and crop yield changes under conservation agriculture, *Glob Chang Biol*, *26*, 3325-3335, doi:10.1111/gcb.15001, 2020.
- 895 Wang, G., Huang, W., Zhou, G., Mayes, M. A., & Zhou, J.: Modeling the processes of soil moisture in regulating microbial and carbon-nitrogen cycling, *Journal of Hydrology*, *585*, doi:10.1016/j.jhydrol.2020.124777, 2020.
- Wang, G., Post, W. M., & Mayes, M. A.: Development of microbial-enzyme-mediated decomposition model parameters through steady-state and dynamic analyses, *Ecological Applications*, *23*, 255-272, doi:10.1890/12-0681.1, 2013.
- 900 Wang, J., Xiong, Z., & Kuzyakov, Y.: Biochar stability in soil: meta-analysis of decomposition and priming effects, *Global Change Biology Bioenergy*, *8*, 512-523, doi:10.1111/gcbb.12266, 2016a.
- Wang, Y. P., Jiang, J., Chen-Charpentier, B., Agosto, F. B., Hastings, A., Hoffman, F., Rasmussen, M., Smith, M. J., Todd-Brown, K., Wang, Y., Xu, X., & Luo, Y. Q.: Responses of two nonlinear microbial models to warming and increased carbon input, *Biogeosciences*, *13*, 887-902, doi:10.5194/bg-13-887-2016, 2016b.
- 905 Wieder, W. R., Bonan, G. B., & Allison, S. D.: Global soil carbon projections are improved by modelling microbial processes, *Nature Climate Change*, *3*, 909-912. 2013.
- Wieder, W. R., Grandy, A. S., Kallenbach, C. M., & Bonan, G. B.: Integrating microbial physiology and physio-chemical principles in soils with the Microbial-MIneral Carbon Stabilization (MIMICS) model, *Biogeosciences*, *11*, 3899-3917, doi:10.5194/bg-11-3899-2014, 2014.
- 910 Wieder, W. R., Grandy, A. S., Kallenbach, C. M., Taylor, P. G., & Bonan, G. B.: Representing life in the Earth system with soil microbial functional traits in the MIMICS model, *Geoscientific Model Development*, *8*, 1789-1808, doi:10.5194/gmd-8-1789-2015, 2015.
- Wieder, W. R., Sulman, B. N., Hartman, M. D., Koven, C. D., & Bradford, M. A.: Arctic soil governs whether climate change drives global losses or gains in soil carbon, *Geophysical Research Letters*, *46*, 14486-14495. 2019.
- 915 Woolf, D., Amonette, J. E., Street-Perrott, F. A., Lehmann, J., & Joseph, S.: Sustainable biochar to mitigate global climate change, *Nat Commun*, *1*, 56, doi:10.1038/ncomms1053, 2010.
- Woolf, D., & Lehmann, J.: Modelling the long-term response to positive and negative priming of soil organic carbon by black carbon, *Biogeochemistry*, *111*, 83-95, doi:10.1007/s10533-012-9764-6, 2012.
- 920 Xia, J. Y., Luo, Y. Q., Wang, Y. P., Weng, E. S., & Hararuk, O.: A semi-analytical solution to accelerate spin-up of a coupled carbon and nitrogen land model to steady state, *Geoscientific Model Development*, *5*, 1259-1271, doi:10.5194/gmd-5-1259-2012, 2012.

- 925 Yan, Z., Bond-Lamberty, B., Todd-Brown, K. E., Bailey, V. L., Li, S., Liu, C., & Liu, C.: A moisture function of soil heterotrophic respiration that incorporates microscale processes, *Nat Commun*, 9, 2562, doi:10.1038/s41467-018-04971-6, 2018.
- Yang, Q., Zhou, H., Bartocci, P., Fantozzi, F., Masek, O., Agblevor, F. A., Wei, Z., Yang, H., Chen, H., Lu, X., Chen, G., Zheng, C., Nielsen, C. P., & McElroy, M. B.: Prospective contributions of biomass pyrolysis to China's 2050 carbon reduction and renewable energy goals, *Nat Commun*, 12, 1698, doi:10.1038/s41467-021-21868-z, 2021.
- 930 Yoo, G., Kim, H., & Choi, J. Y.: Soil Aggregate Dynamics Influenced by Biochar Addition using the ^{13}C Natural Abundance Method, *Soil Science Society of America Journal*, 81, 612-621, doi:10.2136/sssaj2016.09.0313, 2017.
- Zhang, H., Goll, D. S., Wang, Y. P., Ciais, P., Wieder, W. R., Abramoff, R., Huang, Y., Guenet, B., Prescher, A. K., Viscarra Rossel, R. A., Barre, P., Chenu, C., Zhou, G., & Tang, X.: Microbial dynamics and soil physicochemical properties explain large-scale variations in soil organic carbon, *Glob Chang Biol*, doi:10.1111/gcb.14994, 2020.
- 935 Zhang, Y., Sun, C. X., Chen, L., and Duan, Z.: Catalytic potential of soil hydrolases in northeast China under different soil moisture conditions, *Revista de la ciencia del suelo y nutrición vegetal*, 9, 116-124, 2009.
- Zhao, M., & Running, S. W.: Drought-induced reduction in global terrestrial net primary production from 2000 through 2009, *Science*, 329, 940-943, doi:10.1126/science.1192666, 2010.
- 940 Zheng, H., Wang, X., Luo, X., Wang, Z., & Xing, B.: Biochar-induced negative carbon mineralization priming effects in a coastal wetland soil: Roles of soil aggregation and microbial modulation, *Sci Total Environ*, 610-611, 951-960, doi:10.1016/j.scitotenv.2017.08.166, 2018.
- Zhou, H., Zhang, D., Wang, P., Liu, X., Cheng, K., Li, L., Zheng, J., Zhang, X., Zheng, J., Crowley, D., van Zwieten, L., & Pan, G.: Changes in microbial biomass and the metabolic quotient with biochar addition to agricultural soils: A Meta-analysis, *Agriculture Ecosystems & Environment*, 239, 80-89, doi:10.1016/j.agee.2017.01.006, 2017a.
- 945 Zhou, M., Zhu, B., Wang, S., Zhu, X., Vereecken, H., & Bruggemann, N.: Stimulation of N_2O emission by manure application to agricultural soils may largely offset carbon benefits: a global meta-analysis, *Glob Chang Biol*, 23, 4068-4083, doi:10.1111/gcb.13648, 2017b.
- Zimmerman, A. R., Gao, B., & Ahn, M.-Y.: Positive and negative carbon mineralization priming effects among a variety of biochar-amended soils, *Soil Biology and Biochemistry*, 43, 1169-1179, doi:10.1016/j.soilbio.2011.02.005, 2011.
- 950 Zomer, R. J., Xu, J., & Trabucco, A.: Version 3 of the Global Aridity Index and Potential Evapotranspiration Database, *Sci Data*, 9, 409, doi:10.1038/s41597-022-01493-1, 2022.